Tree-shaped Hybrid Fractal Antenna for Biomedical Applications using ANN and PSO

Manpreet Kaur (✉ sketty@rediffmail.com)

    YCoE Punjabi University GKC

Jagtar Singh Sivia

    Yadavindra College of Engineering Department of Electronics and Communication Engineering

---

Research Article

Tree-shaped Hybrid Fractal Antenna for Biomedical Applications using ANN and PSO

Manpreet Kaur[1], Jagtar Singh Sivia[2]

[1]Assistant Professor, Yadavindra College of Engineering, Punjabi University Guru Kashi Campus, Talwandi Sabo, Bathinda, Punjab, India

[2]Professor, Yadavindra College of Engineering, Punjabi University Guru Kashi Campus, Talwandi Sabo, Bathinda, Punjab, India

[1] sketty@rediffmail.com, [2] jagtarsivian@gmail.com

Abstract – In the present scenario, there is a rapid development in the field of designing efficient medical devices for advanced health care purposes. A distinct hybrid fractal approach for designing tree-shaped antenna using artificial neural network (ANN) and particle swarm optimization is explored in this research paper. ANN modelling provides a promising solution, especially for solving various problems that are usually encountered in science and engineering. A Koch–like structure is added to a Giuseppe Peano-like structure for the construction of a parent hybrid shape. The overall volume of the FR4 based designed prototype is 24 x 20 x 1.6 mm^3. The tree-like geometry is excited by a microstrip line feed, placed at the centre axis of the selected substrate. The ground plane dimension 'L$_g$' has been optimized specifically with particle swarm optimization technique. To realize the effectiveness of the hybrid fractal approach, the projected antenna is experimentally analyzed. The designed structure is compact, geometrically appealing and offers sufficient bandwidth. The projected antenna operates over 2.41 to 2.44 GHz, with fundamental frequency of 2.42 GHz. The S11 ≤ -10 dB bandwidth examined at the working frequency is 1.44 % (35.1 MHz). Moreover, the projected antenna offers promising gain and stable radiation patterns at the claimed frequency. A simplified ANN strategy is also utilized for the estimation of selected output parameters. For completeness, simulated, estimated, optimized and experimental responses are reported to examine the reliability of the proposed hybrid fractal approach. Furthermore, the performance is effectively described by analyzing the behavior of projected antenna with different excitation methods. Excellent outcomes validate that this compact device makes it an ideal choice for bimedical applications.

Keywords- Tree-shaped hybrid fractal antenna, Excitation methods, Resonant frequency, Biomedical applications, Bandwidth, Artificial neural network

1. Introduction

The health care industry is advancing rapidly towards the development of robust and efficient antennas [1]. Biomedical applications mainly require miniaturized devices for proper therapeutic and health care monitoring [2,3]. Antennas serve in two important fields related to the biomedical sector such as biotelemetry and biomedical therapy [4]. Biotelemetry involves the measurement of physiological parameters/ conditions of ambulatory patients

over a distance, whereas biomedical therapy focuses on the use of specific medical procedures for the treatment of several mental and/or physiological disorders [5]. Nowadays, glucose monitoring, neurostimulators, endoscopy, defibrillators, and retinal prosthesis, etc are the few examples of medical applications that utilize the facility of remote monitoring [7]. In this multidisciplinary domain, three important fields such as engineering, medicine, and science are merged together to design innovative antennas for better health care facilities [8]. Fractal electromagnetics is a specific area in which electromagnetic theory is fused with the fractal design concept that allows the development of distinct type of antennas, called fractal antennas [9]. A fractal design is specified as a geometrical arrangement with self-similar patterns. Fractal structures follow unique features like self-similarity and space-filling, that result in compact, small size antennas with multiband/wideband functionality [10,11]. The demand of the market for producing small size antennas forces the amalgamation of different fractal configurations with enhanced characteristics [12]. Moreover, this revolutionary innovative hybrid fractal procedure allows the creation of remarkable devices by merging special kinds of fractals with well-defined features [13].

Several fantastic hybrid fractal strategies have been realized in the previous literature [14-18]. Chen et al. [19] have practically realized a novel technique for suitable size reduction. A circularly polarized antenna design based on Koch fractal was experimentally investigated in [20]. Sharma et al. [21] have illustrated a fractal antenna that was manufactured by the concoction of Koch and Hilbert shapes. Results were computed at two different feed locations and then the performance was anticipated. Several nested hexagonal fractal antennas using ring-like pattern were designed with different rotation angles. Fabricated prototypes were analyzed and found that they are beneficial for wireless applications [22]. Nowadays, researchers are showing keen interest in the study and physical realization of antennas designed for biomedical purposes. Various miniaturization strategies related to antennas have been proposed in the past [23-25]. Kaur et al. [26] have clearly described the role of antennas in the biomedical sector. These antennas allow the treatment of several harmful diseases in a much faster and comfortable way. Li et al. [27] have experimentally demonstrated the behavior of a circularly polarized antenna and reported that it is highly effective for Industrial, Scientific and Medical (ISM) band biotelemetry applications. A novel triangular slot antenna was evaluated at 2.45 GHz [28]. An alumina ceramic material based antenna of size 18 x 24 x 0.65 mm^3 was constructed. L-shaped slots were etched from the patch and fed with coplanar waveguide fed structure [29]. Kumar et al. [30] have reported the behavior of an FR4 based dual V-shaped antenna for ISM band applications. In recent years, an artificial neural network (ANN) approach has been successfully utilized in several engineering and optimization problems [31-33]. A vehicle detection system based on a well-known ANN method was proposed for the effective identification of vehicles with sufficient reliability [34]. Dhaliwal et al. [35] have performed a deep experimental analysis of Sierpinski gasket fractal antenna with a widely explored ANN approach. Various performance factors of a circularly polarized antenna fed with distinct excitation methods are presented in [36]. The behavior of recommended structure with few important feeding techniques was investigated in [37]. Rajpoot et al. [38] have utilized a particle swarm optimization (PSO) technique for the optimization of fractional bandwidth of an I-shaped microstrip antenna. Different types of evolutionary algorithms were used for the

implementation of circularly polarized antennas. The results were compared and discussed in [39]. Two types of antennas such as Sierpinski gasket and Koch monopole were analyzed using ANN-PSO [40].

An antenna is considered as a prime constituent of several medical devices because it can communicate robustly with the outside environment [3]. For effective communication, there must be suitable design criteria. This paper considers several aspects of the projected tree-shaped antenna to point out how the hybrid fractal approach is useful in the design process. After a brief and relevant introduction, the paper is structured in the following way: Section 2 reveals the structural details of the projected prototype with two iterations. The geometry of the designed radiator along with a modified ground plane is effectively described. The suggested ANN approach for the prediction of desired parameters is illustrated in Section 3. A brief description regarding PSO algorithm is given in Section 4. Detailed results are elaborated in Section 5, after that the obtained results are compared with previously constructed antennas. At last, Section 6 summarizes the entire design process and the evaluated results of the projected antenna.
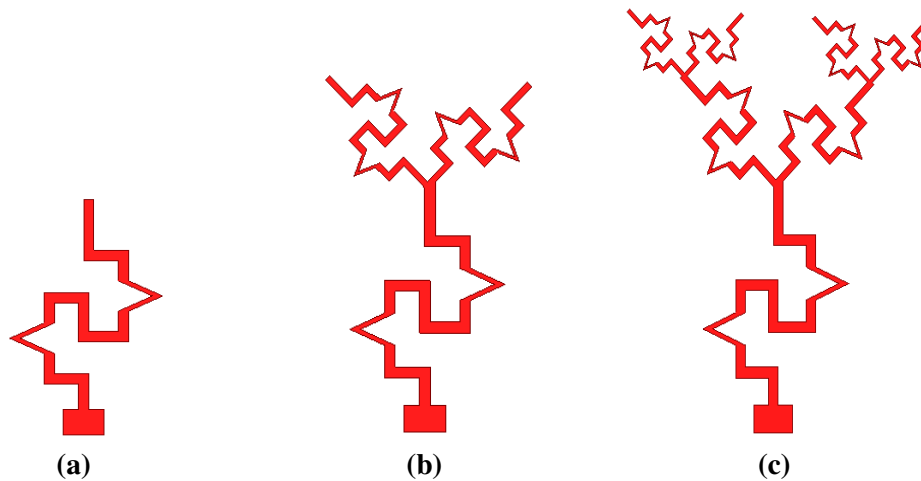
2. Evolution of the Antenna

Fig. 1 Design strategy (a) Generator curve (b) 1st iteration design (c) 2nd iteration design

The projected tree-shaped hybrid fractal antenna is designed by considering two iterations so that it can operate effectively at the preselected frequency [13]. A systematic hybrid fractal approach is employed to demonstrate the design concept. In the present work, the hybrid fractal procedure involves the creation of a compact tree-shaped patch by the concoction of two special kinds of fractals with significant attributes. The whole structure consists of a hybrid fractal tree-shaped patch connected to a rectangular feed line, and a modified ground plane. The Giuseppe Peano and Koch based hybrid curve is derived by amalgamating a Giuseppe Peano and Koch-like structures. This curve is specified as the generator curve, which is also the parent shape of the projected design [16]. Scaling factor of 0.6 is used in the design process. This value helps in controlling the alignment of branches of the tree-shaped antenna. After scaling, this hybrid curve is then applied to every branch of the tree, so as to obtain the final shape. The radiating patch is backed by an easily available FR4 substrate of height 1.6 mm. The basic characteristics of the selected substrate material are dielectric

constant (ε_r) 4.4 and mass density 1900 kg/m³ [17]. The overall volume of this designed prototype is 24 x 20 x 1.6 mm³. Especially, a modified ground plane of 'L_g'= 18 mm and 'W_g' = 20 mm is positioned below the substrate.

Two slots of different shapes are etched from the ground structure, and the dimensions of these slots are finalized after a comprehensive parametric analysis. For the purpose of excitation, a 50-ohm connector is placed at the specified position and is connected with the conducting patch [31]. To fulfill the necessary condition of impedance matching, feed width is chosen as 2.4 mm. Detailed procedure followed during the generation of final geometry is properly illustrated in Figs 1 (a-c). The design parameters of the projected antenna are presented in Table 1. The geometrical configuration of projected tree-shaped hybrid fractal antenna is reported in Fig. 2. Fig 2(a) portrays the final design of patch and Fig 2(b) illustrates the modified ground plane.

Table 1 Geometrical descriptors of projected antenna

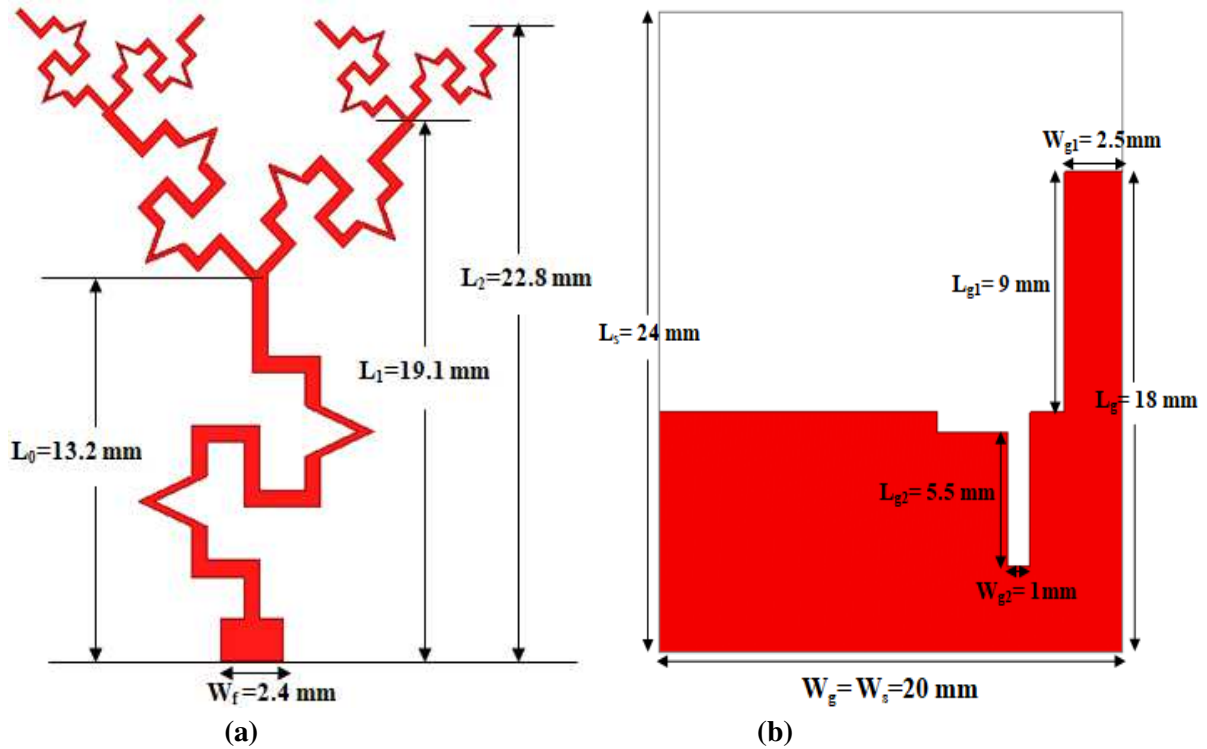| Parameter	Value(mm)
Vertical dimension of 0th iteration 'L_0'	13.2
Vertical dimension of 1st iteration 'L_1'	19.1
Vertical dimension of 2nd iteration 'L_2'	22.8
Horizontal dimension of substrate 'L_s'	24
Vertical dimension of substrate 'W_s'	20
Horizontal dimension of modified ground plane 'W_g'	20
Vertical dimension of modified ground plane 'L_g'	18

Fig. 2 Projected tree-shaped antenna (a) Designed patch (b) Modified ground plane

3. Artificial Neural Network

Artificial neural network is a special type of biologically inspired classification network that can solve complex large scale real-life problems [10]. For efficient functionality, modern technology employs artificial neural networks because these networks are extremely adaptive and have the capability to learn very quickly [32]. ANN has multiple neurons that are arranged in the form of layers. The first layer i.e. input layer is fed with the inputs from the outside world. The intermediate layer i.e. hidden layer performs the required computations and then forwards the output to the next layer [35]. At the last stage, the output layer generates the overall output. In brief, the size of the input layer is determined by the number of actual inputs, and the size of the output layer is specified by the number of outputs to be estimated [41]. The size associated with the hidden layer varies according to the user requirements and is determined by the hit and trial approach. During the training process, weights and threshold values are automatically adjusted by the network so that the computed error exhibits a minimum value [41]. The adjustments are carried out by the backpropagation mechanism. Fig. 3 depicts the suggested feed-forward back propagation artificial neural network (FFBP-ANN) containing three fundamental layers.
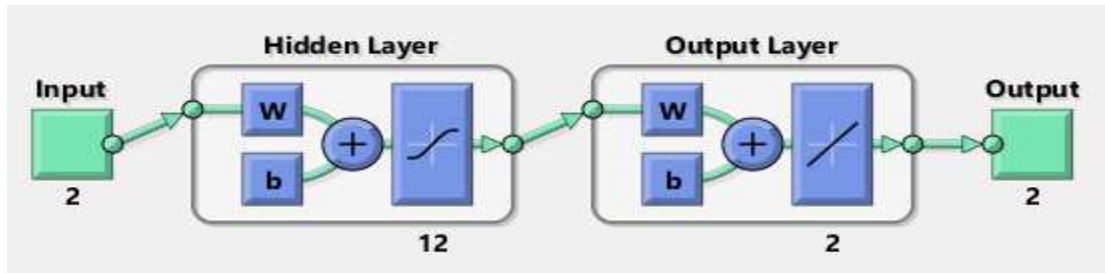

Fig. 3 Suggested FFBP-ANN portraying the three fundamental layers

The suggested FFBP-ANN model has one input layer containing 2 neurons, one hidden layer containing 12 neurons and at the end, one output layer holding 2 neurons. Levenberg-Marquardt algorithm is employed to train the suggested FFBP-ANN network so as to attain a high degree of accuracy [13]. The entire data pool is partitioned into three classes. Each class contains different number of samples. 70% of total samples in data pool are assigned for training the model. Rest 30% of samples are deputed for testing and validation [31]. Training phase in FFBP-ANN considers these steps: transfer the inputs in forward mode, computation and backpropagation of the error value and then weight value adjustments. The transfer functions selected for the hidden and output layers are tangent sigmoid (TANSIG) and pure linear (PURELIN), respectively.

4. Particle Swarm Optimization

Particle swarm optimization (PSO) is a powerful metaheurstic algorithm that was originally proposed by Kennedy and Eberhart in 1995 [16]. This algorithm relies on the cooperative behavior, found naturally in birds, fishes, and insects. Recently, PSO has gained huge attention as it has the capability to efficiently handle complex multidimensional problems related to engineering [38]. In this algorithm, each individual is considered as a 'particle' having no weight and volume. Each particle moves within the multidimensional search space

at a certain speed with reference to its own experience as well as the experience of other particles present nearby [39]. The state vector corresponding to each particle represents the position and velocity. Initially, the state of particles is defined randomly. Depending on the research problem, this algorithm requires different boundary conditions, social and cognitive rates [40]. This method iteratively optimizes the defined research problem based on the fitness function. The fitness function plays an important role in evaluating the best solution.

During the search, there are two important parameters to be considered: first one is 'pbest' i.e. the best solution for each particle and the other one is 'gbest' i.e. the best solution based on the entire population [46]. After obtaining the values of 'pbest' and 'gbest', the updation process is followed using the equations given below [16]:

$$v_i(t+1) = wv_i(t) + c_1r_1[pbest(t) - x_i(t)] + c_2r_2[gbest(t) - x_i(t)] \tag{1}$$

$$x_i(t+1) = x_i(t) + v_i(t+1) \tag{2}$$

where v_i and x_i represents the velocity and position of ith particle, respectively. w signifies the inertial weight. The parameters c_1 and c_2 are the two different types of learning factors. Here w is set to 1. $c_1 = c_2 = 1.5$. The flow chart of PSO is presented in Fig. 4.

4.1 Development of cost function

Cost function is essential for solving the optimization problems. It is defined by considering the target value. Firstly, 40 different geometries of projected tree-shpaed hybrid fractal antenna with different values of ground length 'L_g' are designed and simulated in HFSS software. The selected range of 'L_g' is 12.2 to 20.2 mm. The resonant frequency corresponding to each sample is noted down. Then, by using curve fitting approach in MATLAB software, the mathematical equation of 'f_r' is generated which illustrates the relationship between ground length 'L_g' and resonant frequency 'f_r'. The developed mathematical relation is given in Eq. (3), which is described below [16]:

$$f_r = 2.874\sin(0.1762Lg + 5.001) + 0.4387\sin(0.5223Lg + 2.467) + \\ 0.05189\sin(1.558Lg + 1.359) + 0.03237\sin(1.907Lg + 5.146) \tag{3}$$

$$\text{Cost function} = \sqrt[5]{(2.45 - f_r)^2} \tag{4}$$

The formulated cost function is given in Eq. (4). By using the cost function and the above mentioned PSO approach, it is possible to evaluate the optimum value.

5. Experimental Results and Discussion

In order to present several proofs of the reliability and effectiveness of the projected prototype, results obtained from numerical simulations and experimental measurements are described in this section.
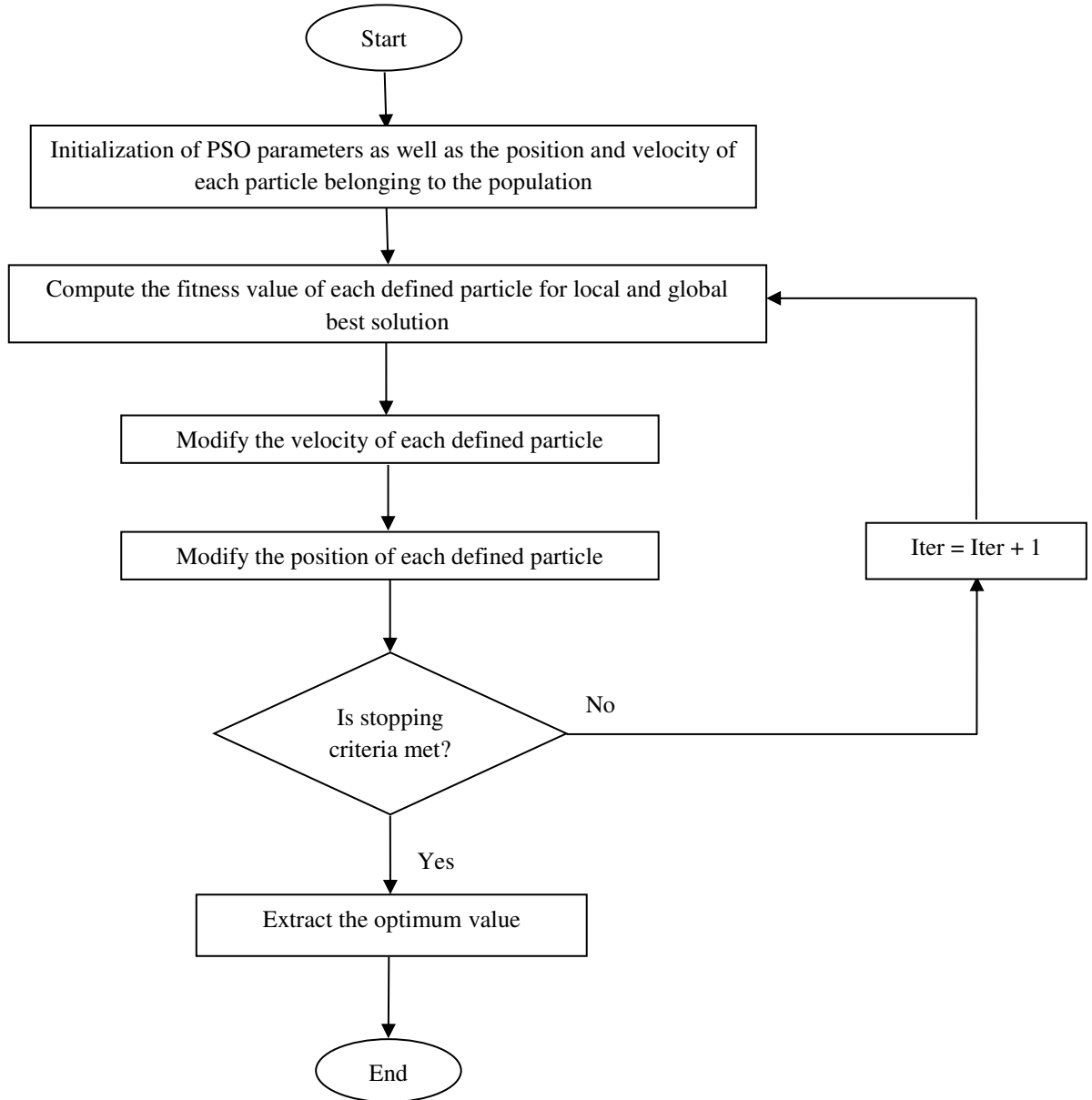
Fig. 4 Detailed flow chart of PSO algorithm [16]

5.1 Projected antenna results

The projected tree-shaped hybrid fractal antenna is modeled in a systematic and accurate way. The design criterion is properly selected by focusing on the desired performance [22]. The antenna must have lower S11 value (≤ -10 dB) and high gain at the frequency of interest. The initial design dimensions of the designed structure are selected and then verified using a finite element method based efficient and high-performance 3D simulator i.e. high-frequency structure simulator (HFSS) software. Simulations up to 2nd iterations are conducted for the effectiveness of the hybrid fractal concept [22]. Enhancement in the electrical length of current flow paths is reported, which allows a reduction in the fundamental operating frequency [31]. For validation purpose, experimental measurements along with simulations are also conducted. The aforementioned antenna is fabricated after computing the results

through simulations. The fabricated device is pictorially represented in Fig. 5. S11 parameters are measured using an Analyzer (Model No. MS46322A) of Anritsu company. It is noted that step by step variation in the generator structure results in improved S11 characteristics. Moreover, Antenna offers design flexibility and size reduction at the claimed frequency band.
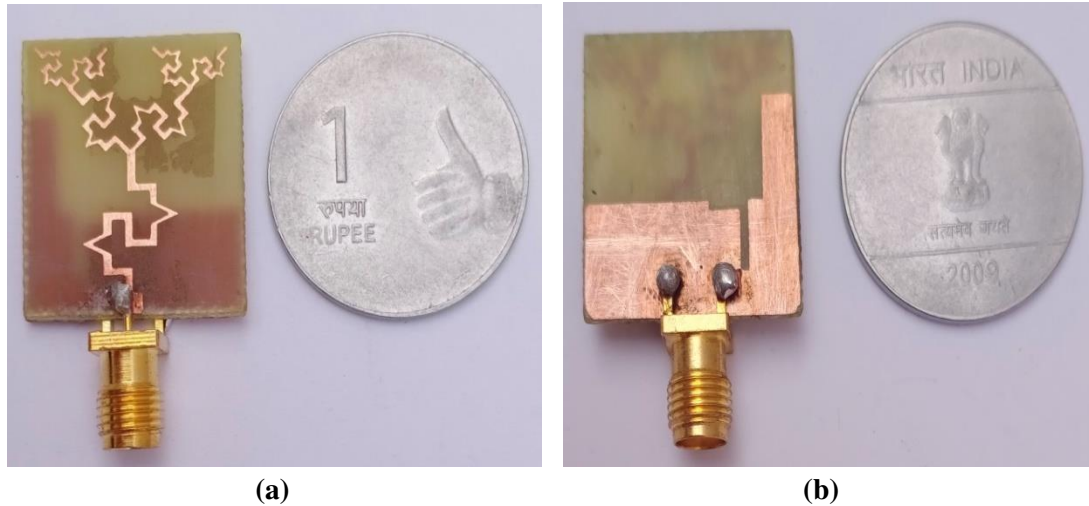

(a)   **(b)**

Fig. 5 Fabricated tree-shaped hybrid fractal antenna   (a) Front view (b) Rear view

Table 2 Results obtained after simulations and experimental measurements

Parameter	Simulated	Measured
Working frequency range (GHz)	2.43-2.46	2.41-2.44
Fundamental frequency (GHz)	2.45	2.42
Bandwidth (MHz)	35.9 (1.46 %)	35.1 (1.44 %)
S11 (dB)	-21.01	-15.09

To aid better understanding, final results of the projected hybrid fractal antenna obtained through simulations and experimental testing are revealed in Table 2. The resonant frequency observed during simulation is 2.45 GHz, whereas the value of fundamental frequency examined during the measurement is 2.42 GHz [18]. The observed value of VSWR is within the acceptable limit (VSWR ≤ 2) at the working frequency [32]. Fig. 6 shows the S11 plot containing simulated and experimentally measured values. Measured bandwidth compresses to 35.1 MHz, compared with simulated bandwidth of 35.9 MHz. Moreover, the antenna gain examined at the frequency of interest is 3.69 dB. Minor deviations in the evaluated results are mainly due to fabrication inconsistencies [35]. The designed antenna when tilted by 5^0 to the left, provides a gain of 1.23 dB and S11 value less than -10 dB at 2.42 GHz. Similarly, when the same antenna is tilted by 5^0 to the right, it shows a resonance at 2.44 GHz with gain 1.39 dB. At this frequency, the S11 value investigated is -18.53 dB. Fig. 7 shows the S11 plot after tilting (5^0 left and right) the designed structure. The results of both antennas after tilting by selected angle are compared with the reported results of the antenna placed at the original position [22]. It is found that the antenna at the original position (projected structure) shows better results in terms of gain.
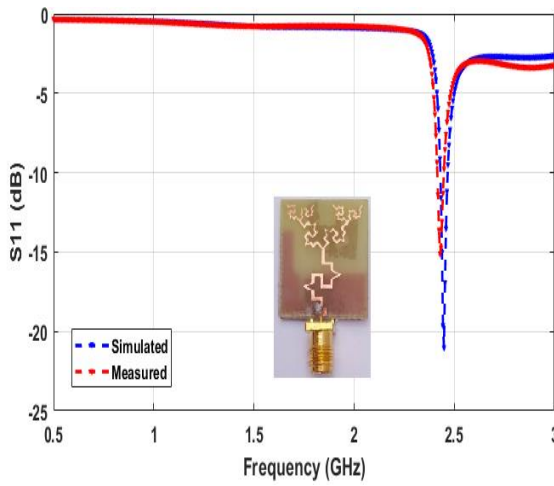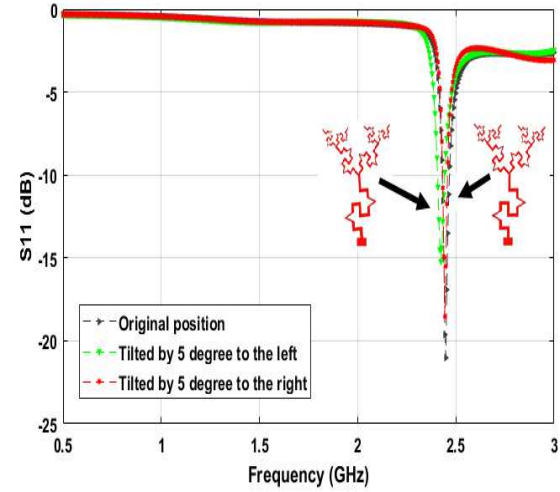
Fig. 6 S11 behavior of projected antenna

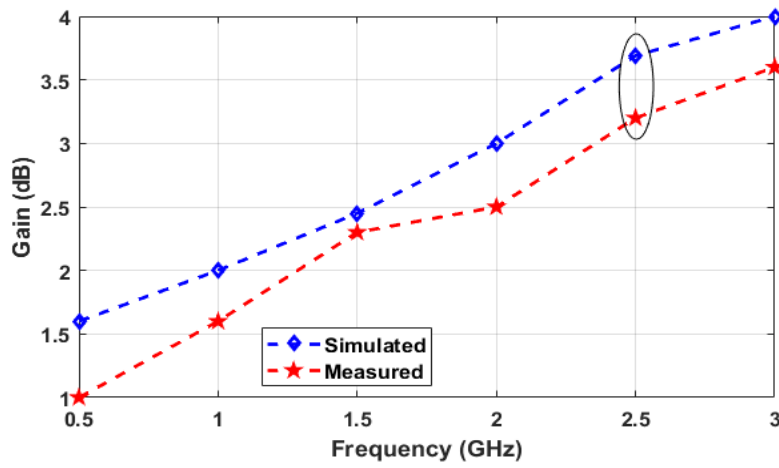**Fig. 7** S11 behavior after tilting the antenna
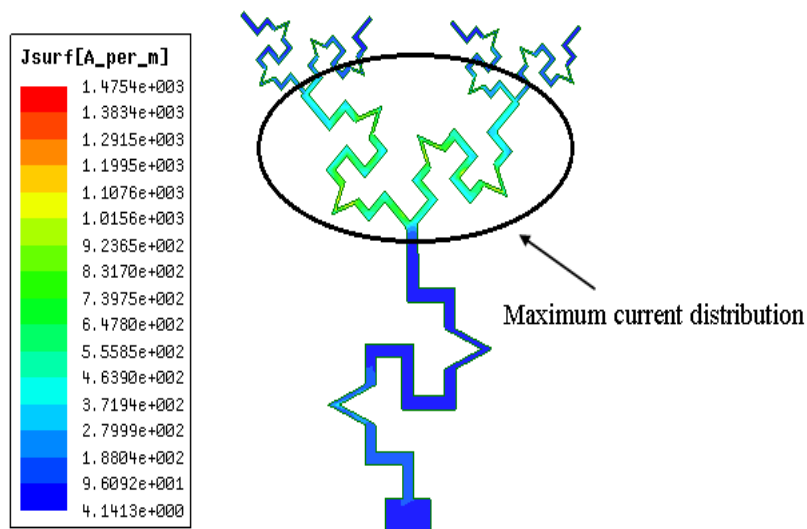

Fig. 8 Gain vs frequency plot

Fig. 9 Current distribution on a designed prototype at 2.45 GHz

A gain of 3.69 dB is examined at the fundamental design frequency. The values of the gain computed after simulations and experimental testing are shown in Fig. 8. The current

distribution on the radiating patch of the designed prototype at 2.45 GHz is illustrated in Fig. 9. The computed current distribution on the designed patch is 1.4754e+003 A per meter at the realized frequency. There is a large current distribution at the portion lies above the middle of the conducting patch i.e. the encircled region [18]. Maximum flow of current is from the endpoint of the generator curve to the top of the structure through all the branches [21]. The projected antenna placed in anechoic chamber is shown in Fig. 10. Fig. 11 demonstrates the radiation patterns for 2nd iterated tree-shaped hybrid fractal antenna in E and H planes. The experimental responses about radiation patterns are collected by performing measurements in an anechoic chamber. The shape of the radiation pattern examined in E-plane is nearly bidirectional, whereas the shape examined in H-plane is bidirectional. Minor distortions are also observed in the patterns. The radiation characteristics are highly satisfactory according to the requirements of medical systems [31]. Therefore, it can be stated that the compact structure with favorable characteristics is well suitable for health care purposes.
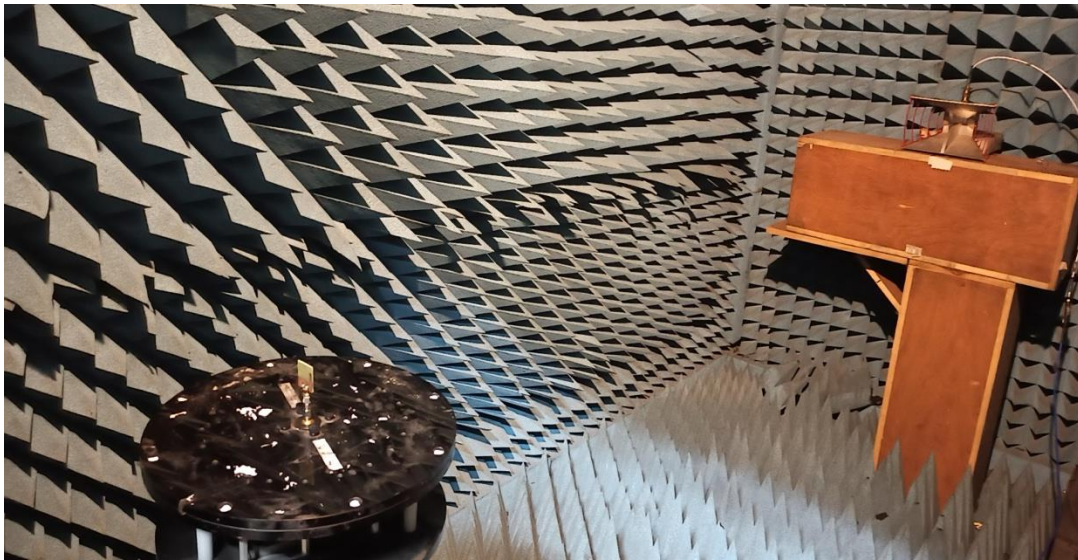

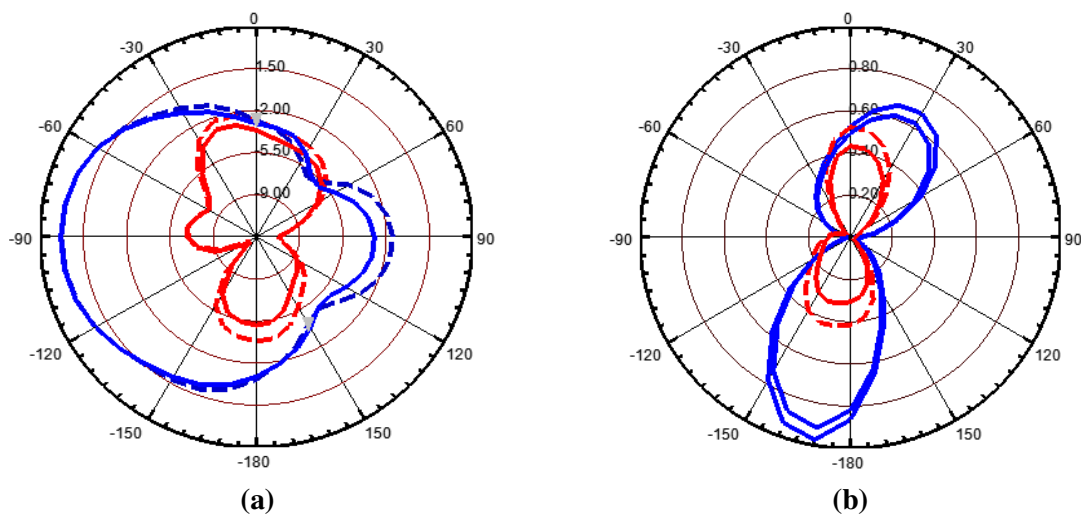**Fig. 10** Projected antenna placed in an anechoic chamber

(a)

(b)

Fig. 11 Simulated (bold lines) and measured (dashed lines) radiation patterns for 2nd iteration of projected implantable antenna at 2.45 GHz. The patterns illustrate the co-(red line) and cross-polar (blue line) components and evaluated at $\Phi= 0^0$ and $\Phi= 90^0$

5.2 Suggested FFBP-ANN model results

The FFBP-ANN trained with Levenberg-Marquardt algorithm is preferred for the estimation of desired antenna performance parameters. A data pool of 25 antennas is used for the behavioral analysis of projected implantable antenna [18]. Each antenna is designed with different dimensions of the substrate ('l_s' and 'w_s'), and then simulated results are interpreted [31]. The neural network results are analyzed in MATLAB software. The FFBP-ANN is fed with two inputs i.e. 'l_s' and 'w_s' and the parameters predicted at the output of network are 'f_r' and 'g'. The values of resonant frequency 'f_r' and gain 'g' are noted down. The value of 'l_s' lies in between 23.5 to 27.5 mm and the value of 'w_s' is in the range of 20 to 26 mm. The FFBP-ANN is trained several times so as to achieve accurate outputs. TANSIG and PURELIN are the selected activation functions associated with the hidden and output layer, respectively [32]. Fig. 12 specifies the performance plot of FFBP-ANN based on the Levenberg-Marquardt algorithm. This plot provides the best outcomes for validation, testing, and training. It is worth mentioned that the best validation performance examined from a performance plot is 0.0089208 at epoch 12 from a total of 18 epochs. Fig 13 illustrates the comparison of target and FFBP-ANN outputs. Table 3 reveals the comparison of simulated and FFBP-ANN outputs (resonant frequency and gain) in tabular form. Fig 14 depicts the plot of absolute error related to 'f_r' and Fig. 15 graphically represents the absolute error related to 'g'.
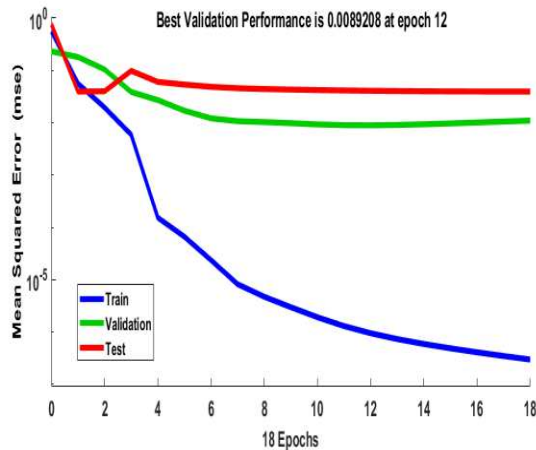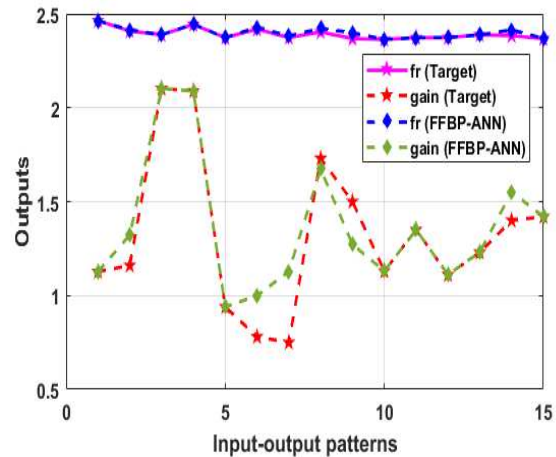

Fig. 12 Performance plot of FFBP-ANN model

Fig. 13 Target and FFBP-ANN outputs

Table 3 Comparison of simulated and FFBP-ANN outcomes

S.no	Dimensions of substrate		Target output		FFBP-ANN output		Errors corresponding to	
	L_s	W_s	f_r	gain	f_r	gain	f_r	gain
1	23.5	20	2.4639	1.127	2.4636	1.1265	0.0002	0.0004
2	24.5	20	2.4088	1.16	2.4145	1.3219	-0.005	-0.1619
3	25	20	2.3888	2.1023	2.3889	2.1024	-0.0001	-0.0001
4	23.5	21.5	2.4439	2.09	2.4450	2.0898	-0.0011	0.0001
5	25	22	2.3737	0.94	2.3733	0.9398	0.0003	0.0001
6	24	20.5	2.4188	0.78	2.4283	0.9986	-0.0095	-0.2186
7	25	21.5	2.3737	0.75	2.3823	1.1284	-0.0086	-0.3784
8	24	22	2.4038	1.73	2.4225	1.6737	-0.0188	0.0562

9	25.5	23	2.3687	1.5	2.3995	1.2716	-0.0308	0.2283
10	26	23	2.3637	1.13	2.3638	1.1298	-0.0001	0.0001
11	27	24	2.3737	1.35	2.3727	1.3501	0.0009	-0.0001
12	24.5	24	2.3737	1.11	2.3746	1.1105	-0.0009	-0.0005
13	25	25	2.3888	1.23	2.3876	1.2305	0.00117	-0.0005
14	24.5	25.5	2.3838	1.4	2.4148	1.5509	-0.0310	-0.1509
15	25	25.5	2.3687	1.42	2.3696	1.4204	-0.0009	-0.0004
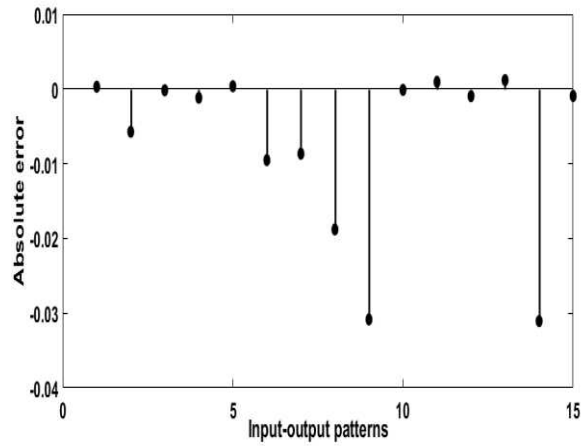
Fig. 14 Absolute error related to 'f_r'
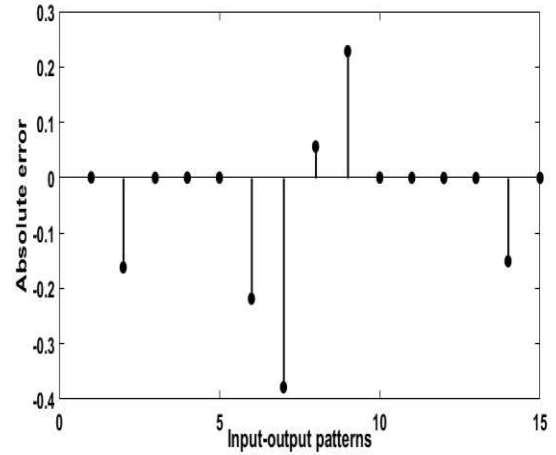
Fig. 15 Absolute error related to 'g'

Table 4 Performance determined by FFBP-ANN

	Training	**Testing**	**Validation**
Mean square error	9.48e-7	4.07e-2	8.29e-3
Regression	0.99	0.97	0.99

The performance behavior of suggested FFBP-ANN is judged on the basis of absolute error and mean square error. Absolute error provides knowledge about the quality of training, whereas mean square error measures the mean of the squared difference between the targets and actual outputs [32]. The value of mean square error indicates the effectiveness of the network. Table 4 gives the performance determined by the suggested FFBP-ANN model. In narrow sense, it is suggested that the FFBP-ANN model is an effective tool for the prediction of selected antenna performance parameters.

5.3 PSO results

In this work, particle swarm optimization technique is employed during the designing of projected tree-shaped antenna. This method helps in achieving the optimized value of ground plane length'L_g'. In this algorithm, the population size chosen is 40 and maximum iterations are set to 80 [16]. Proper upper and lower bounds are provided during computation. The formulated cost function generates 17.70 mm as the optimized value of 'L_g'. The best cost value obtained is 2.0784e-04. This value of ground length successfully proves the applicability of the suggested algorithm according to the design problem and requirements. The plot of best cost is shown in Fig. 16.
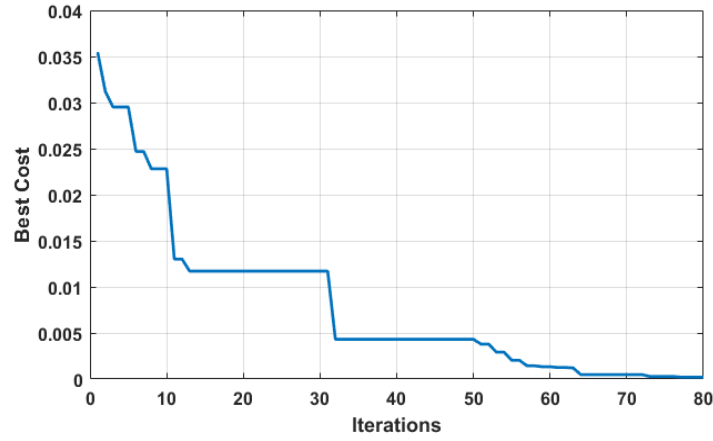
Fig. 16 Variations of Best cost with iterations

5.4 Impact of different excitations methods

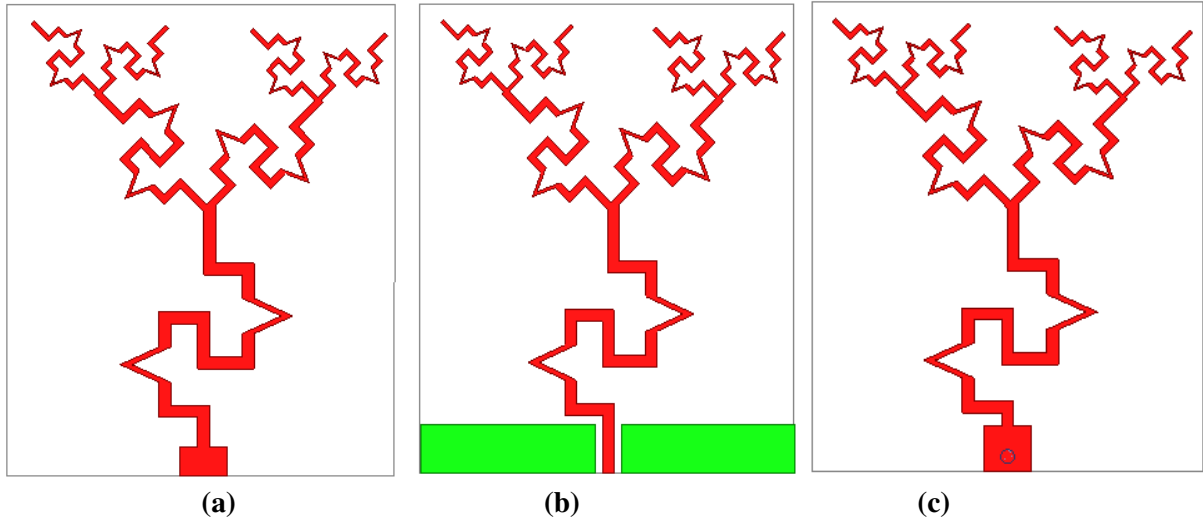(a)   (b)   (c)

Fig. 17 Projected antenna with (a) Microstrip line feed (b) Coplanar waveguide feed (c) Coaxial feed

Feeding mechanism plays an important role in the antenna design process as it helps to reduce the reflections by providing proper impedance matching [36]. Its main function is to effectively couple the input signal to the device under consideration. Selection of an appropriate excitation method is a crucial task as it requires deep knowledge about the designing criteria involved in all excitation methods that are considered in this study [37]. The excitation criteria affect the input impedance and other important characteristics associated with the device. In this work, three types of excitation methods are chosen: microstrip, coplanar waveguide and coaxial probe [42]. It is worth mentioned that during the designing of proposed geometry with different excitation methods, same dielectric material and simulation tool are used. Fig. 17 reveals the projected prototype with different excitation methods. In coplanar waveguide (CPW)-fed structure, identical ground planes are placed symmetrically on both sides of the CPW line. The length and width of the symmetrical ground structure are 2.5 and 9.3 mm, respectively. The coaxial probe feed is located near the bottom of the designed antenna. The behavior of the proposed hybrid fractal antenna with different excitation methods is analyzed and then the generated results are compared. By doing this, the best excitation method is evaluated

according to the design requirements. The projected tree-shaped hybrid fractal antenna with different feeds are designed and simulated individually. The details of the chosen excitation methods are presented in Table 5.

Table 5 Design details of different feeds

Feed Type	Parameter	Value (mm)
Microstrip line **Fig. 13(a)**	Feed length	1.5
	Feed width	2.4
Coplanar waveguide **Fig. 13(b)**	Length of symmetrical ground	2.5
	Width of symmetrical ground	9.3
	Gap between feed and ground	0.4
Coaxial probe **Fig. 13(c)**	Position along x-axis (from bottom)	1.25
	Position along y-axis	0.0(origin)
	Inner circle diameter	0.7
	Outer circle diameter	1.5

The detailed description of the S11behavior of projected prototype with three different excitation techniques is revealed in Fig. 18. The investigated simulated results of the tree-shaped hybrid fractal antenna with different excitation techniques are summarized in Table 6. It is noted that there are entirely different outcomes. After comparing these outcomes, it is stated that microstrip feed gives favorable performance as per the design requirements.
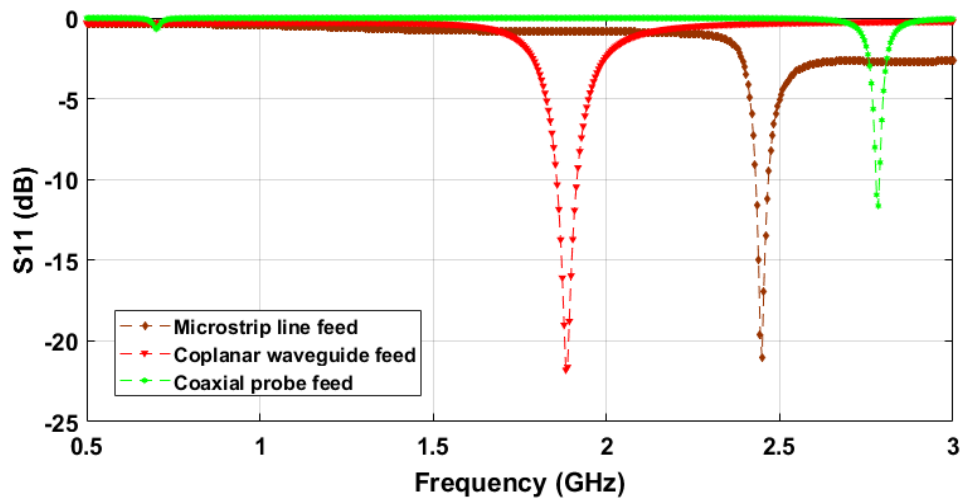
Fig. 18 S11 plot with different excitation techniques

Table 6 Performance characteristics with different excitation techniques

Feeding type	Working frequency (GHz)	Working frequency Range (GHz)	S11 (dB)	Bandwidth (MHz)	Gain (dB)	Radiation Pattern
Microstrip line	2.45	2.4310-2.4669	-21.01	35.9	3.69	Nearly bidirectional
Coaxial probe	2.78	2.7744 -2.7890	-11.63	14.6	-11.99	Nearly omnidirectional
Coplanar waveguide	1.88	1.8500-1.9150	-21.61	65	0.82	Bidirectional

Table 7 Comparison of projected tree-shaped antenna with previously developed antennas

Ref. no.	Substrate type	Volume (mm³)	Operating frequency band	Designed structure
[2]	Rogers 3210	10240	402-405 MHz (MICS band)	Spiral shaped radiator
[3]	FR4	1624	2.45 ISM band	U shaped meandered slotted patch
[4]	Rogers 3210	643	402-405 MHz (MICS band)	Π shaped patch along with two L strips
[5]	Arlon 1000	1524	402-405 MHz (MICS band) 2.4-2.48 GHz (ISM band)	Multilayered model and split ring resonator based patch
[6]	FR4	588	2.4-2.48 GHz (ISM band)	Slotted patch
[7]	Rogers 3210	1265.6	402-405 MHz (MICS band) 2.4-2.48 GHz (ISM band)	Serpentine geometry
[25]	FR4	1925.6	2.45 GHz (ISM band)	Two sleeve patch geometry
[30]	FR4	1478.4	900-915 MHz (ISM band) 2.37-2.55 GHz ISM band)	Dual V shaped patch
[43]	FR4	2897.2	402-406 MHz (MICS band) 2.4-2.5 GHz (ISM band)	Spiral shaped patch
[44]	FR4	9242	2.45 ISM band	Rectangular patch with inset feed
[45]	Copper clad	992	2.4-2.5 GHz (ISM band)	Rectangular shaped patch
Projected antenna	FR4	768	2.45 ISM band	Tree-shaped hybrid fractal patch

Table 7 reveals the comparison of the projected antenna with few antennas that are found in previous literature. The parameters considered for comparison are substrate type, volume, operating frequency band and type of the designed antenna. Each designed prototype is of different shape and size. Some antennas cover two biomedical bands like Medical Implant Communication Service (MICS) and Industrial, Scientific and Medical (ISM). Based on this comparison, it is clear that the projected hybrid fractal antenna satisfies the necessary requirements of medical systems, in perspective to S11 characteristics, gain, and radiation pattern. Here, it is worth mentioned that designed hybrid fractal biomedical device is a strong claimant for health care applications.

6. Conclusion

In this paper, ANN and PSO based tree-shaped hybrid fractal structure which is visually appealing, is practically analyzed for health care applications. PSO approach is employed to obtain the optimum value of ground length. Radiation characteristics, gain, and bandwidth are acceptable according to the biomedical sector requirements. The antenna is suitably matched with VSWR ≤ 2 in the desired operating band. It is examined that measured -10 dB bandwidth is 1.44 % for the operating band (2.41-2.44 GHz). Apart from this, the antenna provides bidirectional radiation patterns with suitable gain value. The developed ANN model effectively shows its suitability for the prediction of antenna output parameters like operating resonant frequency and gain. The designed prototype which is experimentally realized can effectively support medical systems.

References

[1]   A. K. Srinivasan and T. Shanmuganantham, "Analysis and design of implantable Z-monopole antennas at 2.45 GHz ISM Band for biomedical applications," Microwave and Optical Technology Letters, Vol. 57, Issue 2, pp. 468-473, Feb 2015

[2]   J. Kim and Y. Rahmat-Samii, "Implantable antennas inside a human body: simulations, designs and characterizations," IEEE Transactions on Microwave Theory and Techniques, Vol. 52, No. 8, pp. 1934-1943, 2004

[3]   S. Sukhija and R. K. Sarin, "A U-Shaped Meandered Slot Antenna for Biomedical Applications," Progress in Electromagnetics Research M, Vol. 62, pp. 65-77, Jan 2017

[4]   C. M. Lee, T. C. Yo, F. J. Huang and C. H. Luo, "Dual-resonant π-shape with double L-strips PIFA for implantable biotelemetry," Electronics Letters, Vol. 44, No. 14, pp. 837-839, Feb 2008

[5]   C. J. S. Fernandez, O. Q. Teruel, J. R. Carrion, L. I. Sanchez and E. R. Iglesias, "Dual-band microstrip patch antenna based on short-circuited ring and spiral resonators for implantable medical devices," IET Microwave Antennas & Propagation, Vol. 4, No. 8, pp. 1048-1055, Sept 2010

[6]   S. A. Kumar and T. Shanmuganantham, "Implantable CPW-fed rectangular patch antenna for ISM band biomedical applications," International Journal of Microwave and Wireless Technologies, Vol. 6, Issue 1, pp. 101-107, Feb 2014

[7]   T. Karacolak, A. Z. Hood and E. Topsakal, "Design of a Dual-Band Implantable Antenna and Development of Skin Mimicking Gels for Continuous Glucose Monitoring," IEEE Transactions of Microwave Theory and Techniques, Vol. 56, Issue 4, pp. 1001-1008, May 2008

[8]   S. Bhattacharjee and S. Maity, "Miniaturization of MEMs-Based Smart Patch Antennas for Biomedical Applications," Proceedings of the International Conference on Recent Cognizance in Wireless Communication & Image Processing, Jaipur, pp. 279-285, 16-17 Jan 2015

[9]   Y. K. Choukiker, S. K. Sharma and S. K. Behera, "Hybrid Fractal Shape Planer Monopole Antenna Covering Multiband Wireless Communications with MIMO Implementation for Handheld Mobile Devices," IEEE Transactions on Antennas and Propagation, Vol. 62, No. 3, pp. 1483-1488, Mar 2014

[10]   J. S. Sivia, A. P. S. Pharwaha and T. S. Kamal, "Analysis and Design of Circular Fractal Antenna using Artificial Neural Networks," Progress In Electromagnetics Research B, Vol. 56, pp. 251-267, Nov 2013

[11]   A. Sundaram, M. Maddela and R. Ramadoss, "Koch-Fractal Folded-Slot Antenna Characteristics," IEEE Antennas and Wireless Propagation Letters, Vol. 6, pp. 219-222, April 2007

[12] I. K. Bangi and J. S. Sivia, "Minkowski and Hilbert Curves Based Hybrid Fractal Antenna for Wireless Applications," International Journal of Electronics and Communications, Vol 85, pp. 159-168, Feb 2018

[13] M. Kaur and J. S. Sivia, "ANN and FA Based Design of Hybrid Fractal Antenna for ISM Band Applications," Progress in Electromagnetics Research C, Vol. 98, pp. 127-140, Jan 2020

[14] K. Kaur and J. S. Sivia, "A Compact Hybrid Multiband Antenna for Wireless Applications," Wireless Personal Communications, Vol 97, Issue 4, pp. 5917-5927, Dec 2017

[15] C. Jain and S. Singh, "Feed Point Optimization of Koch-Minkowski Hybrid Boundary antenna for ISM Band," Wireless Personal Communications, Vol. 108, Issue 4, pp. 2403-2414, May 2019

[16] M. Kaur and J. S. Sivia, "Minkowski, Giuseppe Peano and Koch Curves based Design of Compact Hybrid Fractal Antenna for Biomedical Applications using ANN and PSO," International Journal of Electronics and Communications, Vol. 99, pp. 14-24, Feb 2019

[17] I. K. Bangi and J. S. Sivia, "Moore, Minkowski and Koch Curves Based Hybrid Fractal Antenna for Multiband Applications," Wireless Personal Communications, Vol. 108, Issue 4, pp. 2435-2448, May 2019

[18] M. Kaur and J. S. Sivia, "Giuseppe Peano and Cantor set fractals based miniaturized hybrid fractal antenna for biomedical applications using artificial neural network and firefly algorithm," International Journal of RF and Microwave Computer-Aided Engineering, Vol. 30, Issue 1, pp. 1-11, Nov 2019

[19] W. L. Chen, G. M. Wang and C. X. Zhang, "Small-Size Microstrip Patch Antenna Combining Koch and Sierpinski Fractal-Shapes," IEEE Antennas and Wireless Propagation Letters, Vol. 7, pp. 738-741, July 2008

[20] A. Farswan, A. K Gautam, B. K. Kanaujia and K. Rambabu, "Design of Koch Fractal Circularly Polarized Antenna for Handheld RFID Reader Applications," IEEE Transactions on Antennas and Propagation, Vol. 64, Issue 2, pp. 1-6, Jan 2015

[21] N. Sharma and S. S. Bhatia, "Double split labyrinth resonator-based CPW-fed hybrid fractal antennas for PCS/UMTS/WLAN/Wi-Max applications," Journal of Electromagnetic Waves and Applications, Vol. 33, Issue 18, pp. 2476-2498, Dec 2019

[22] N. Sharma and S. S. Bhatia, "Performance enhancement of nested hexagonal ring-shaped compact multiband integrated wideband fractal antennas for wireless applications," International Journal of RF and Microwave Computer-Aided Engineering, Vol. 30, Issue 3, pp. 1-21, Dec 2019

[23] S. Das and D. Mitra, "Design of a compact circular polarized implantable ring slot antenna for biomedical applications," Electromagnetics, Vol. 40, Issue 2, pp. 1-10, Feb 2020

[24] S. A. Kumar and T. Shanmuganantham, "Analysis and design of CPW fed antenna at ISM band for biomedical applications," Alexandria Engineering Journal, Vol. 57, Issue 2, pp. 723-727, June 2018

[25] S. Sukhija and R. K. Sarin, "Design and performance of two-sleeve low profile antenna for bio-medical applications," Journal of Electrical Systems and Information Technology, Vol. 4, Issue 1, pp. 49-61, May 2017

[26] G. Kaur, A. Kaur, G. K. Toor, B. S. Dhaliwal and S.S. Pattnaik, "Antennas for biomedical applications," Biomedical Engineering Letters, Vol. 5, Issue 3, pp. 203-212, Sept 2015

[27] H. Li, Y. X. Guo and S. Xiao, "Broadband circularly polarized implantable antenna for biomedical applications," Electronics Letters, Vol. 52, No. 7, pp. 504-506, April 2016

[28] S. A. Kumar and T. Shanmuganantham, "Coplanar waveguide-fed ISM band implantable crossed-type triangular slot antenna for biomedical applications," International Journal of Microwave and Wireless Technologies, Vol. 6, No. 2, pp. 167-172, April 2014

[29] A. K. Srinivasan and T. Shanmuganantham, "Design of Implantable CPW fed Monopole Antenna for ISM Band Applications," Transactions on Electrical and Electronic Materials, Vol. 15, No. 2, pp. 55-59, April 2014

[30] S. A. Kumar and T. Shanmuganantham, "CPW fed monopole implantable antenna for 2.45 GHz ISM band applications," International Journal of Electronics Letters, Vol. 3, Issue 3, pp. 152-159, May 2014

[31] M. Kaur and J. S. Sivia, "ANN-based Design of Hybrid Fractal Antenna for Biomedical Applications," International Journal of Electronics, Vol. 106, Issue 8, pp. 1184-1199, March 2019

[32] B. S. Dhaliwal and S. S. Pattnaik, "BFO-ANN ensemble hybrid algorithm to design compact fractal antenna for rectenna system," International Journal on Neural Computing and Applications, Vol. 28, Issue 1, pp. 917-928, Dec 2017

[33] K. Sabanci, A. Kayabasi, A. Toktas and E. Yigit, "Notch antenna analysis: Artificial neural network-based operating frequency estimator," Applied Computational Electromagnetics Society Journal, Vol. 32, No. 4, pp. 303-309, April 2017

[34] S. Mantri and D. Bullock, "Analysis of feedforward-backpropagation neural networks used in vehicle detection," Transportation Research Part C: Emerging Technologies, Vol. 3, Issue 3, pp. 161-174, June 1995

[35] B. S. Dhaliwal and S. S. Pattnaik, "Artificial Neural Network Analysis of Sierpinski Gasket Fractal Antenna: A Low-Cost Alternative to Experimentation," Advances in Artificial Neural Systems, Vol. 2013, No. 3, pp. 1-7, Oct 2013

[36] A. A. Nour, F. Fezai and T. Monediere, "Comparison of different feeding techniques of a low-profile dual-band circularly polarized microstrip antenna," European Conference on Antennas and Propagation (EuCAP), April 2016

[37] A. Kumar, J. Kaur and R. Singh, "Performance Analysis of Different Feeding Techniques," International Journal of Emerging Technology and Advanced Engineering, Vol. 3, Issue 3, pp. 884-890, March 2013

[38] V. Rajpoot, D. K. Srivastava and A. K. Saurabh, "Optimization of I-shape Microstrip patch antenna using PSO and curve fitting," Journal of Computational Electronics, Vol. 13, Issue 4, pp. 1010-1013, Dec 2014

[39] A. Deb, J. S. Roy and B. Gupta, "Performance Comparison of Differential Evolution, Particle Swarm Optimization and Genetic Algorithm in the Design of Circularly

Polarized Microstrip Antennas," IEEE Transactions on Antennas and Propagation, Vol. 62, Issue 8, pp. 3920-3928, Aug 2014

[40] Anuradha, A. Patnaik and S. N. Sinha, "Design of Custom-Made Fractal Multi-Band Antennas Using ANN-PSO," IEEE Antennas and Propagation Magazine, Vol. 53, Issue 4, pp. 94-101, Aug 2011

[41] V. V. Thakare and P. K. Singhal, "Bandwidth analysis by introducing slots in microstrip antenna design using ANN," Progress In Electromagnetics Research M, Vol. 9, pp. 107-122, Jan 2009

[42] C. A. Balanis, "Antenna Theory: Analysis and design," 3rd Edition, John Wiley & Sons, London

[43] M. Salim and A. Pourziad, "A Novel Reconfigurable Spiral-Shaped Monopole Antenna for Biomedical Applications," Progress In Electromagnetics Research Letters, Vol. 57, pp. 79-84, Oct 2015

[44] R. Caliskan, S. S. Gultekina, D. Uzer and O. Dundar, "A Microstrip Patch Antenna Design for Breast Cancer Detection," Procedia - Social and Behavioral Sciences 195, pp. 2905-2911, July 2015

[45] S. Shrestha, M. Agarwal, P. Ghane and K. Varahramyan, "Flexible Microstrip Antenna for Skin Contact Application," International Journal of Antennas and Propagation, Vol 2012, July 2012

[46] B. S. Dhaliwal and S. S. Pattnaik, "Development of PSO-ANN Ensemble Hybrid Algorithm and Its Application in Compact Crown Circular Fractal Patch Antenna Design", International Journal on Wireless Personal Communications, Vol. 96, Issue 1, pp. 135-152, Sept 2017

Figures
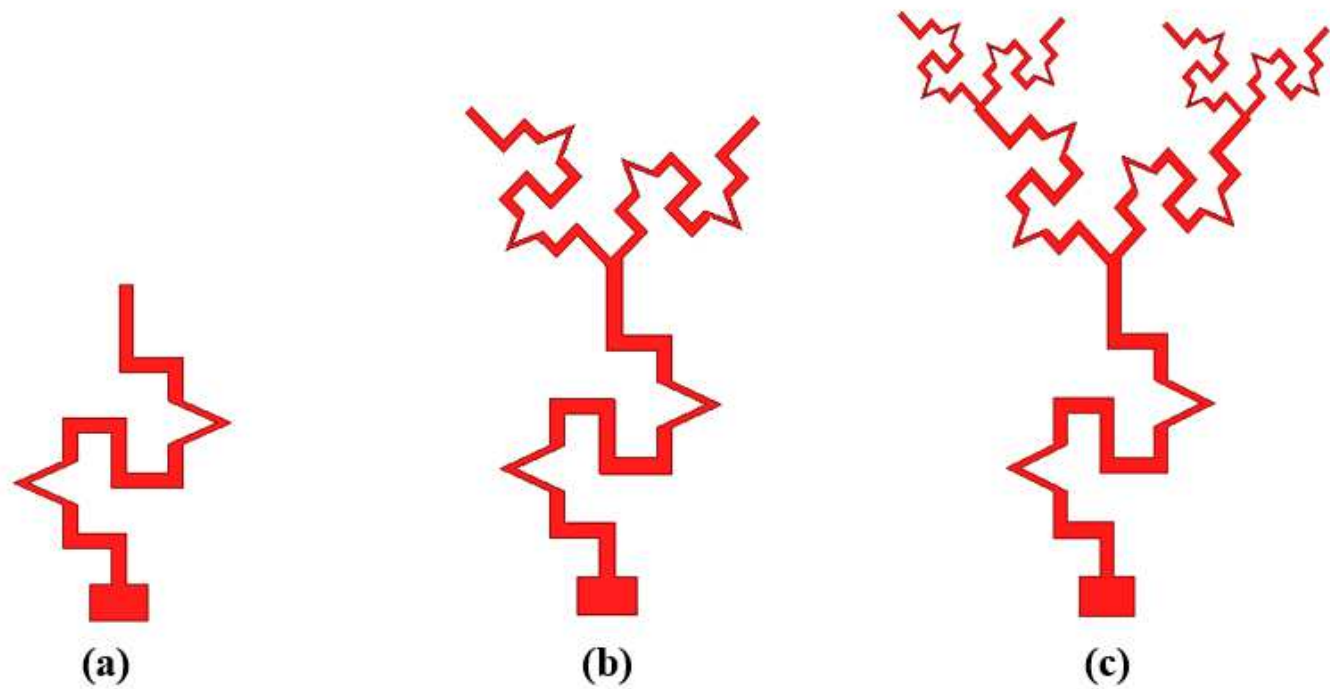
Figure 1

Design strategy (a) Generator curve (b) 1st iteration design (c) 2nd iteration design
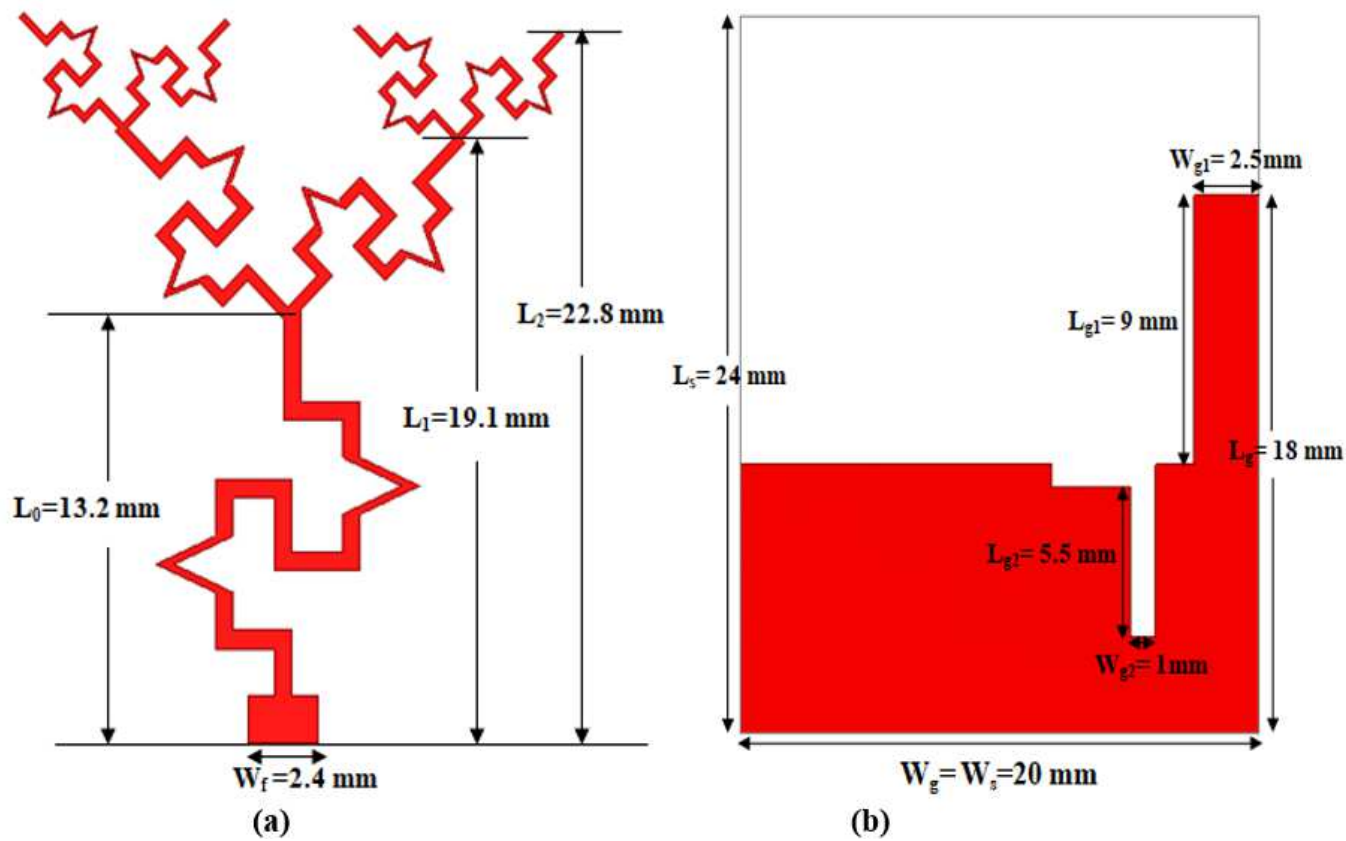
Figure 2

Projected tree-shaped antenna (a) Designed patch (b) Modified ground plane
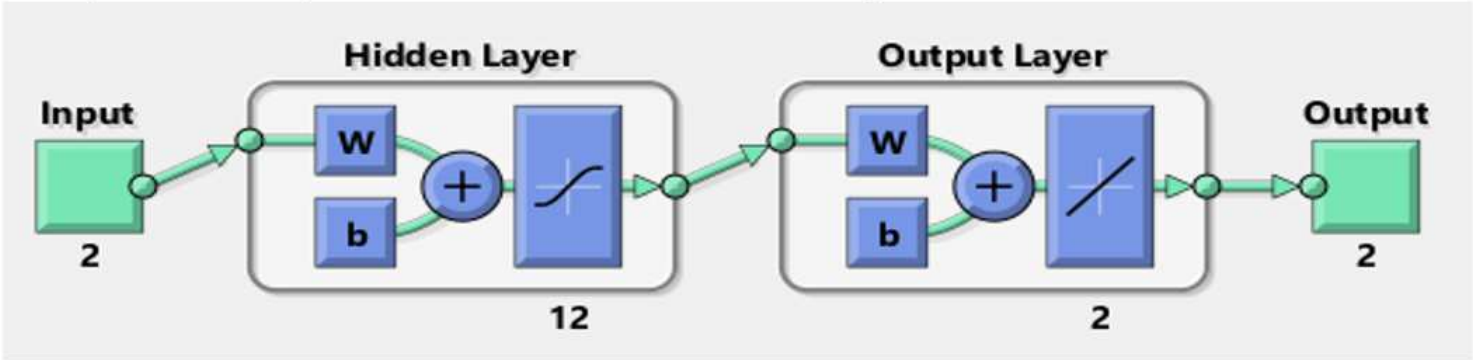
Figure 3

Suggested FFBP-ANN portraying the three fundamental layers
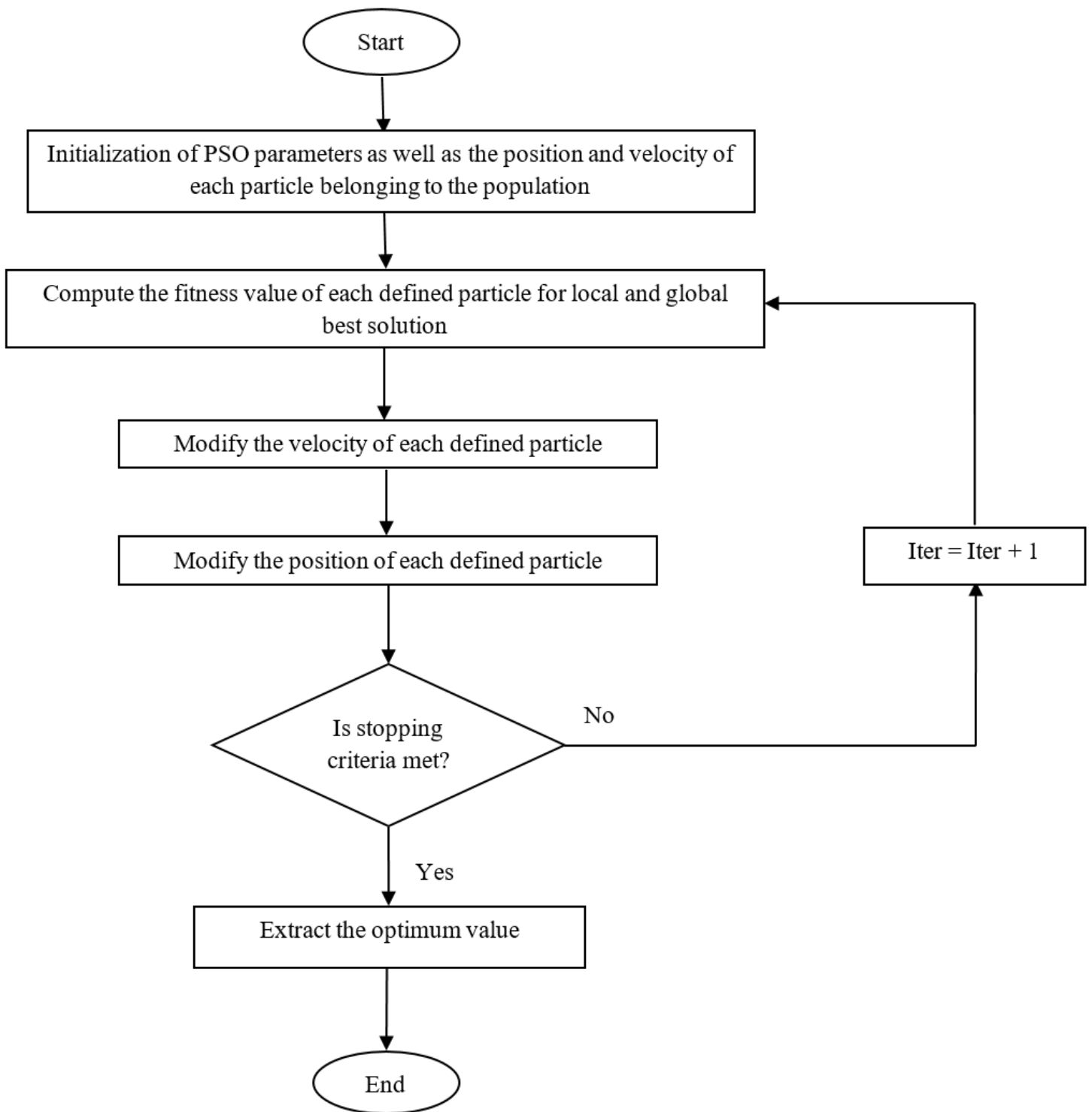
Figure 4

Detailed flow chart of PSO algorithm [16]
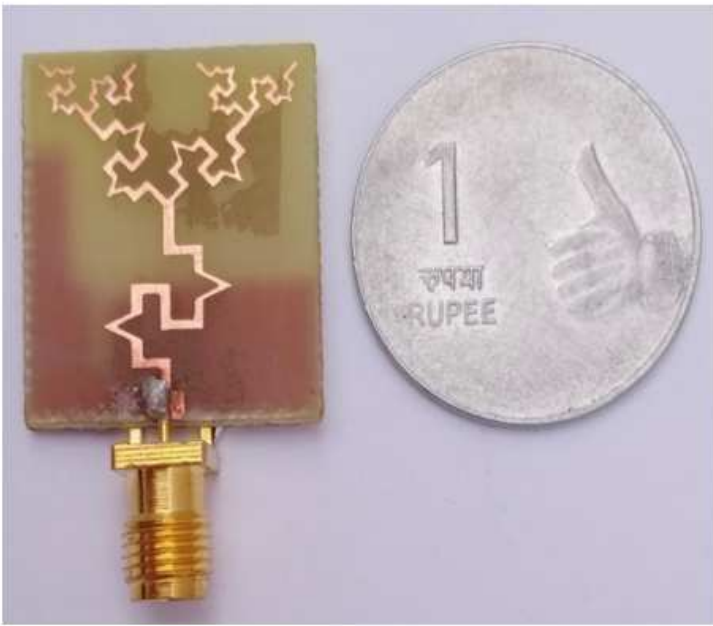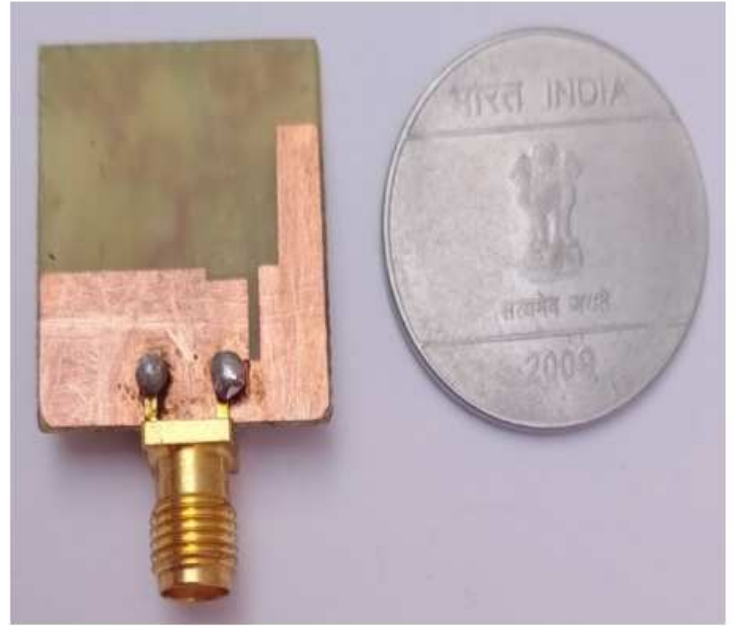
Figure 5

Fabricated tree-shaped hybrid fractal antenna (a) Front view (b) Rear view
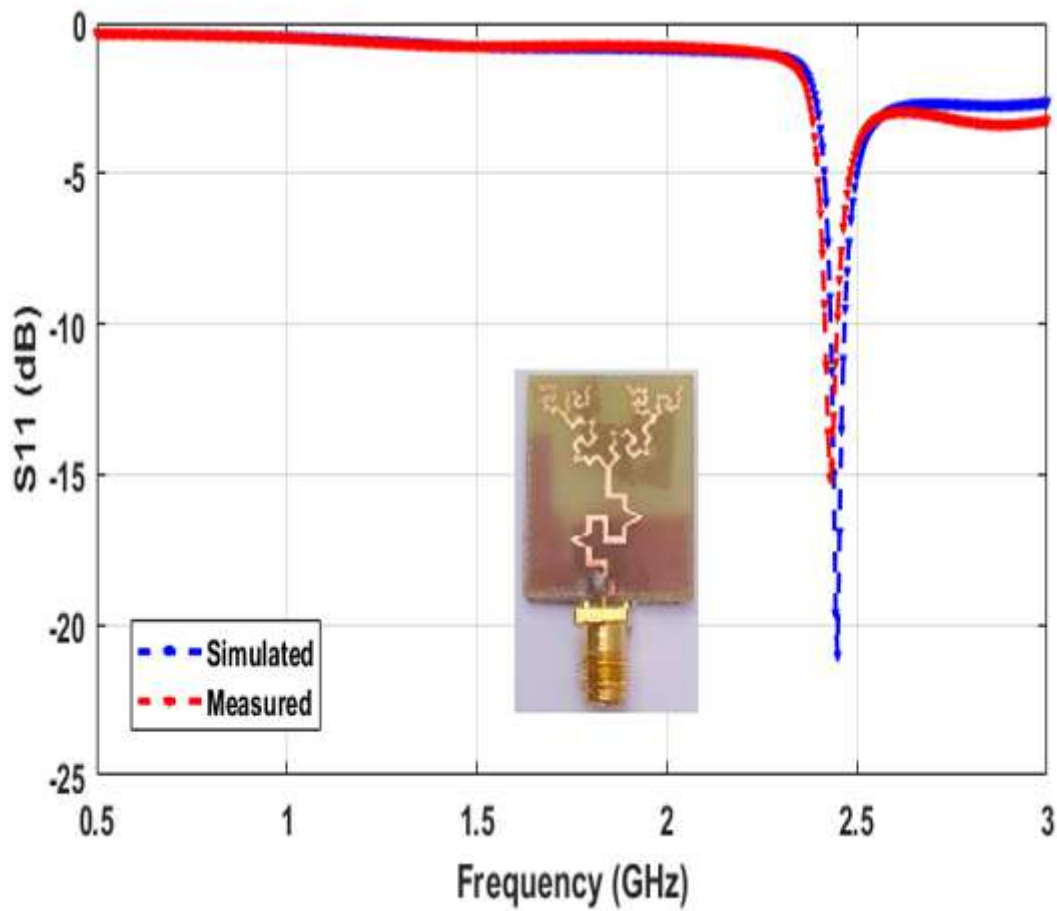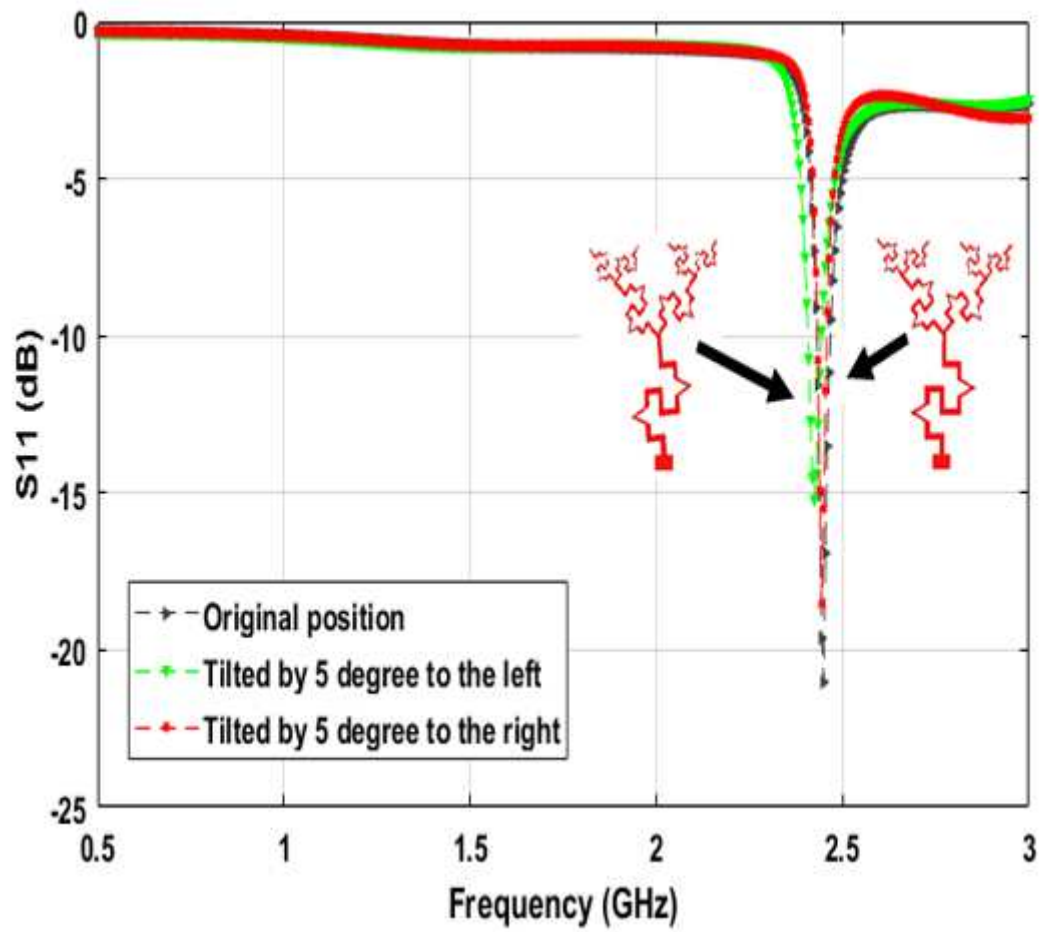

Figure 6

S11 behavior of projected antenna

Figure 7

S11 behavior after tilting the antenna
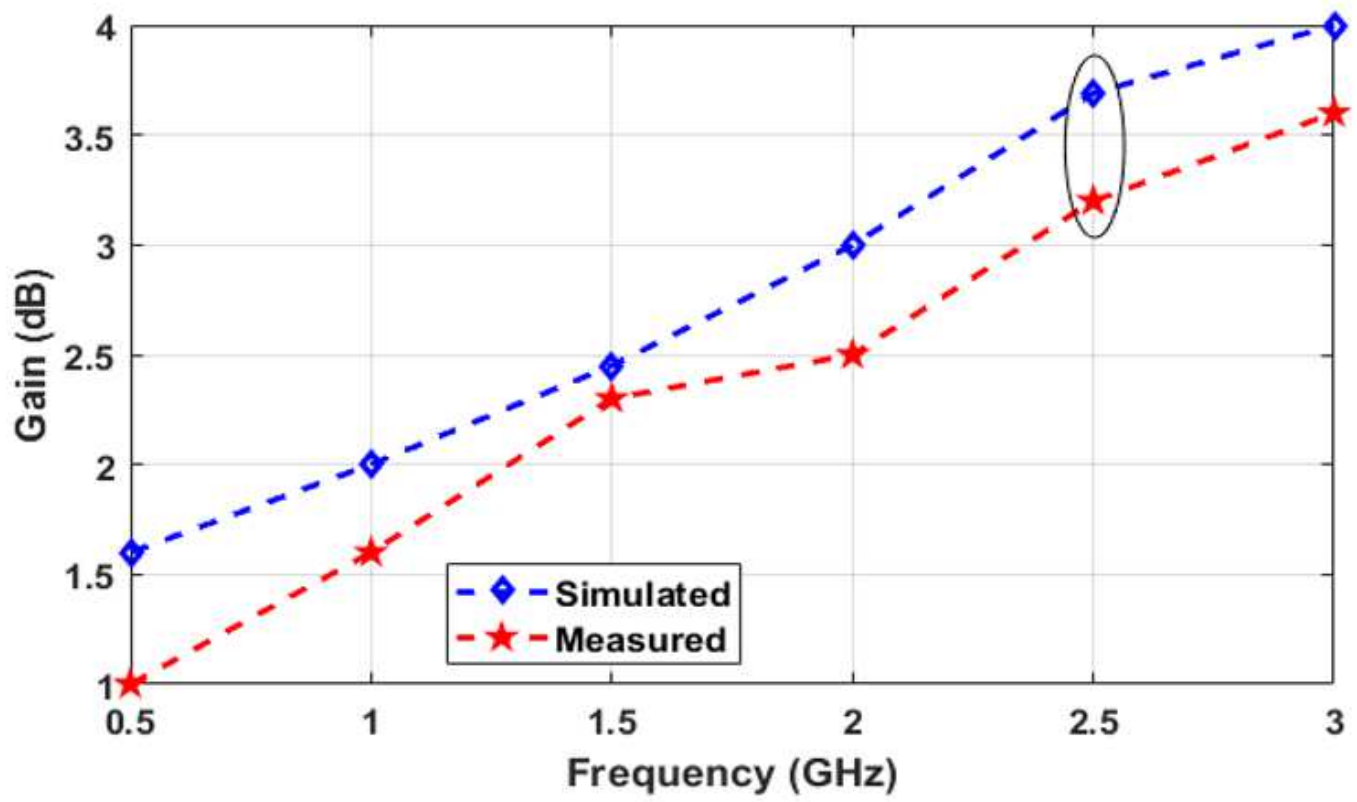
Figure 8

Gain vs frequency plot
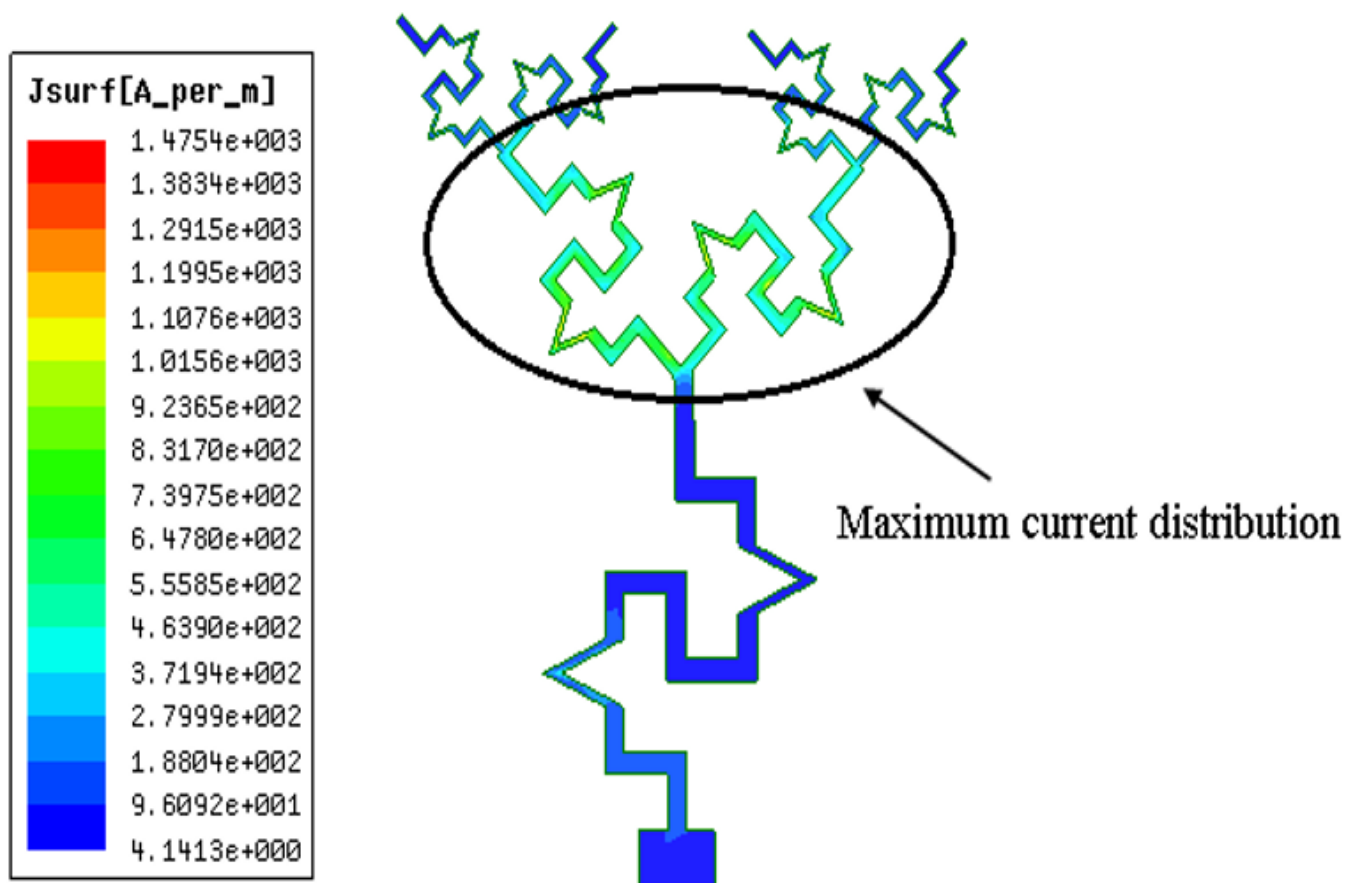
Figure 9

Current distribution on a designed prototype at 2.45 GHz
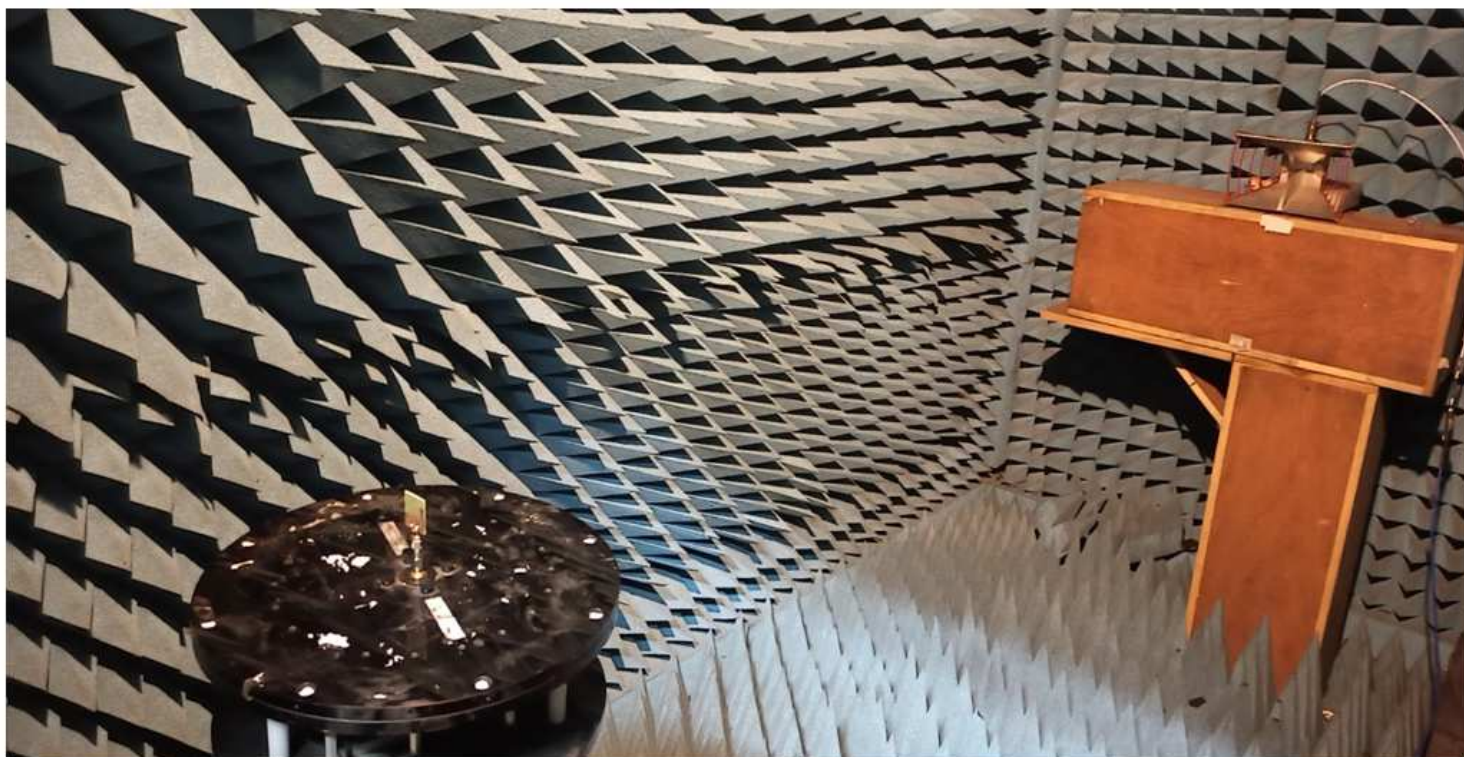
Figure 10

Projected antenna placed in an anechoic chamber

(a)   (b)
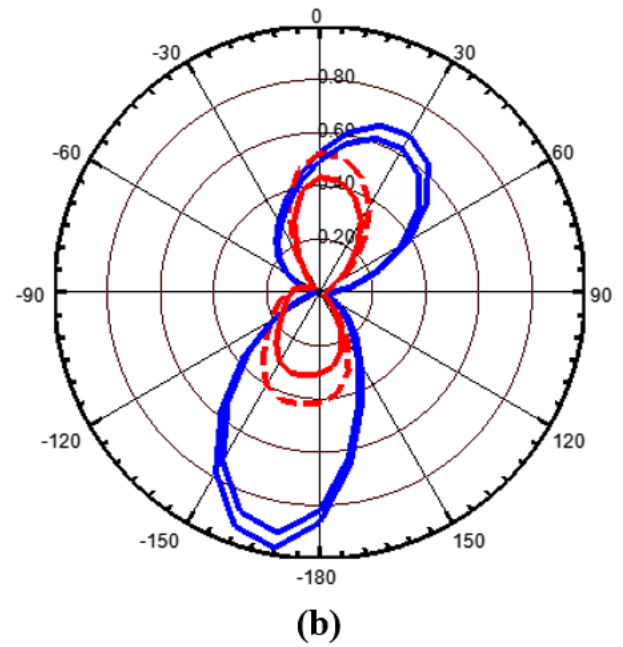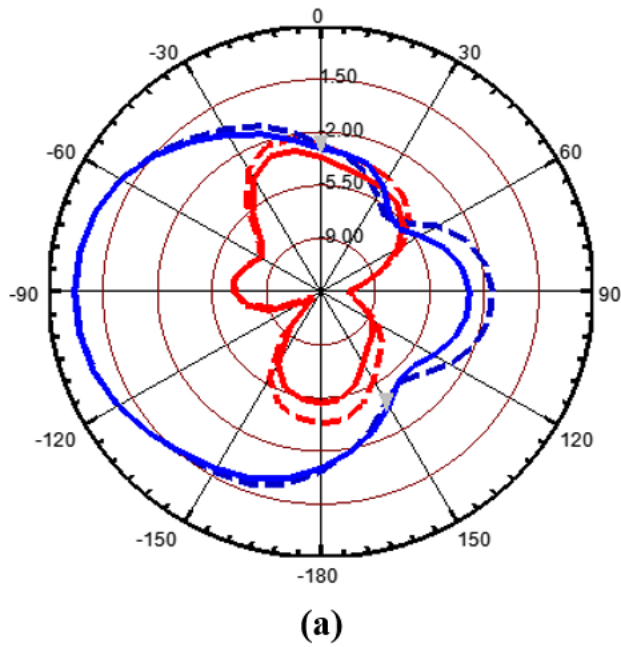
Figure 11

Simulated (bold lines) and measured (dashed lines) radiation patterns for 2nd iteration of projected implantable antenna at 2.45 GHz. The patterns illustrate the co-(red line) and cross-polar (blue line) components and evaluated at Φ= 00 and Φ= 900
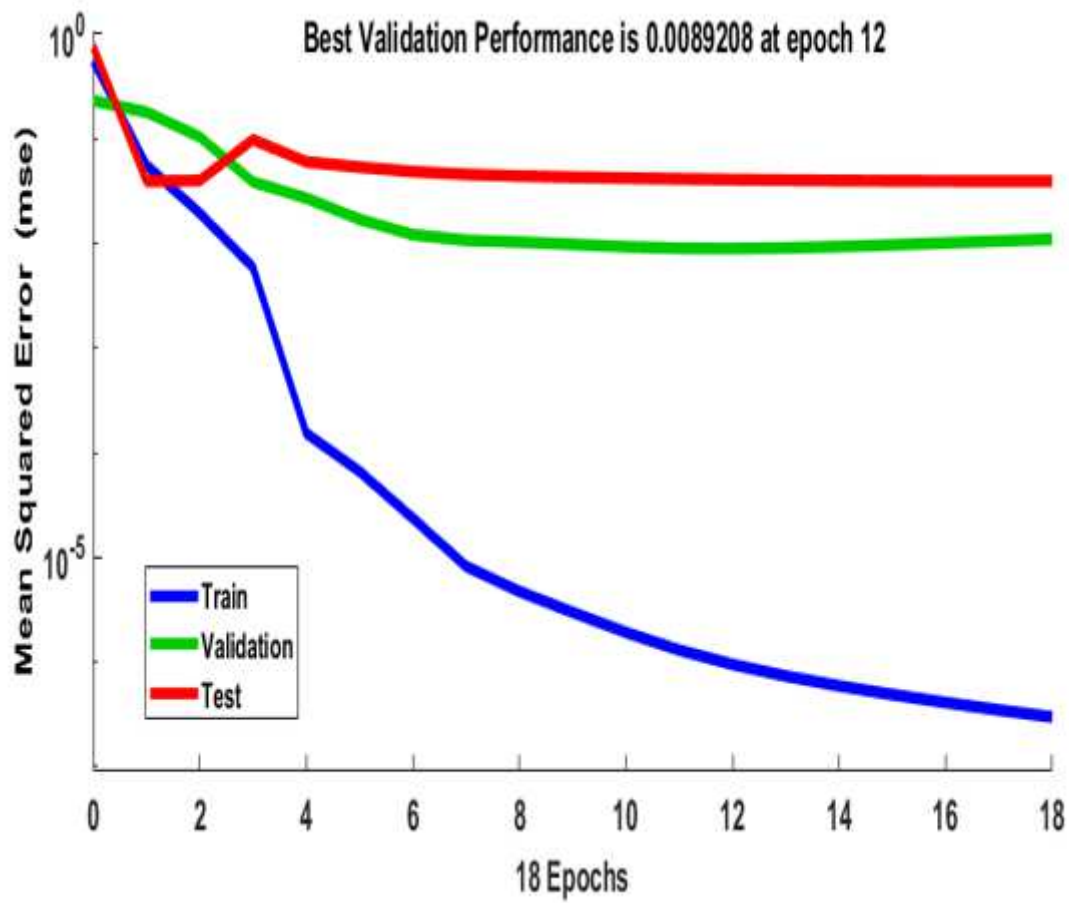
Figure 12

Performance plot of FFBP-ANN model
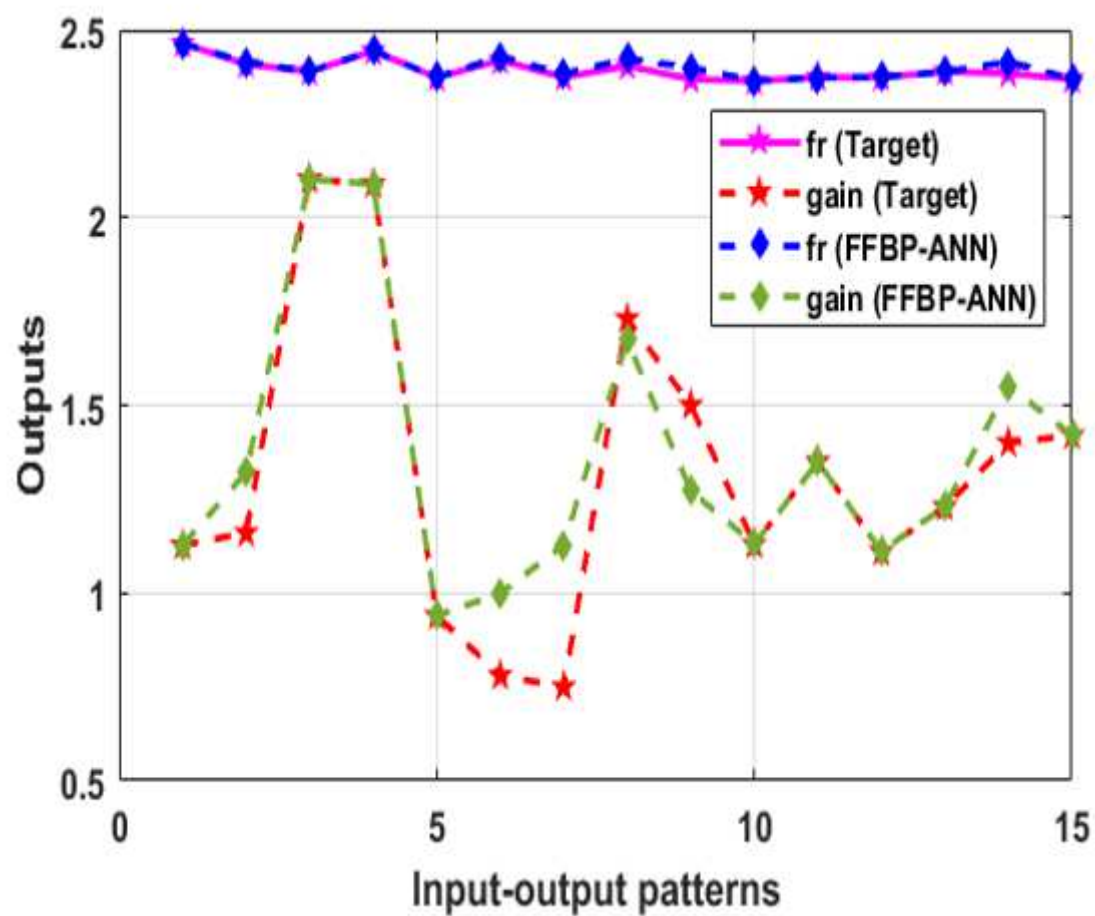
Figure 13

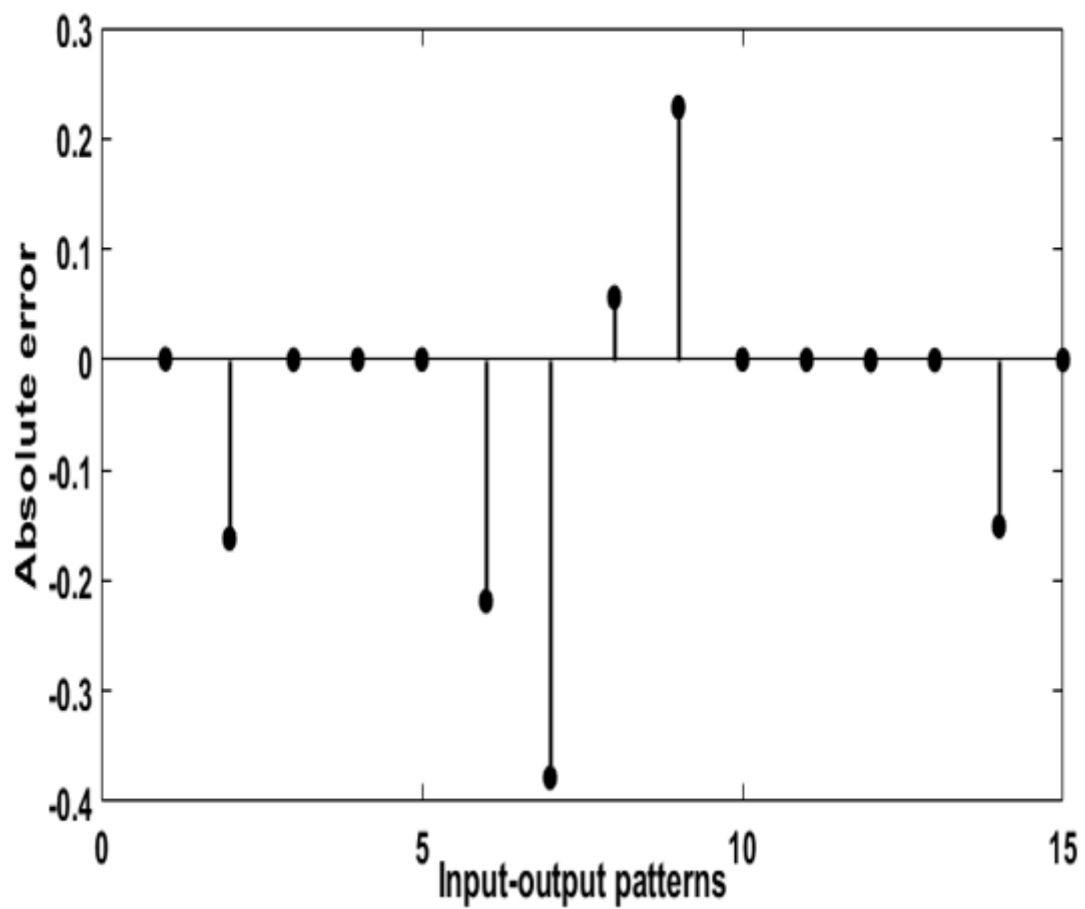Target and FFBP-ANN outputs
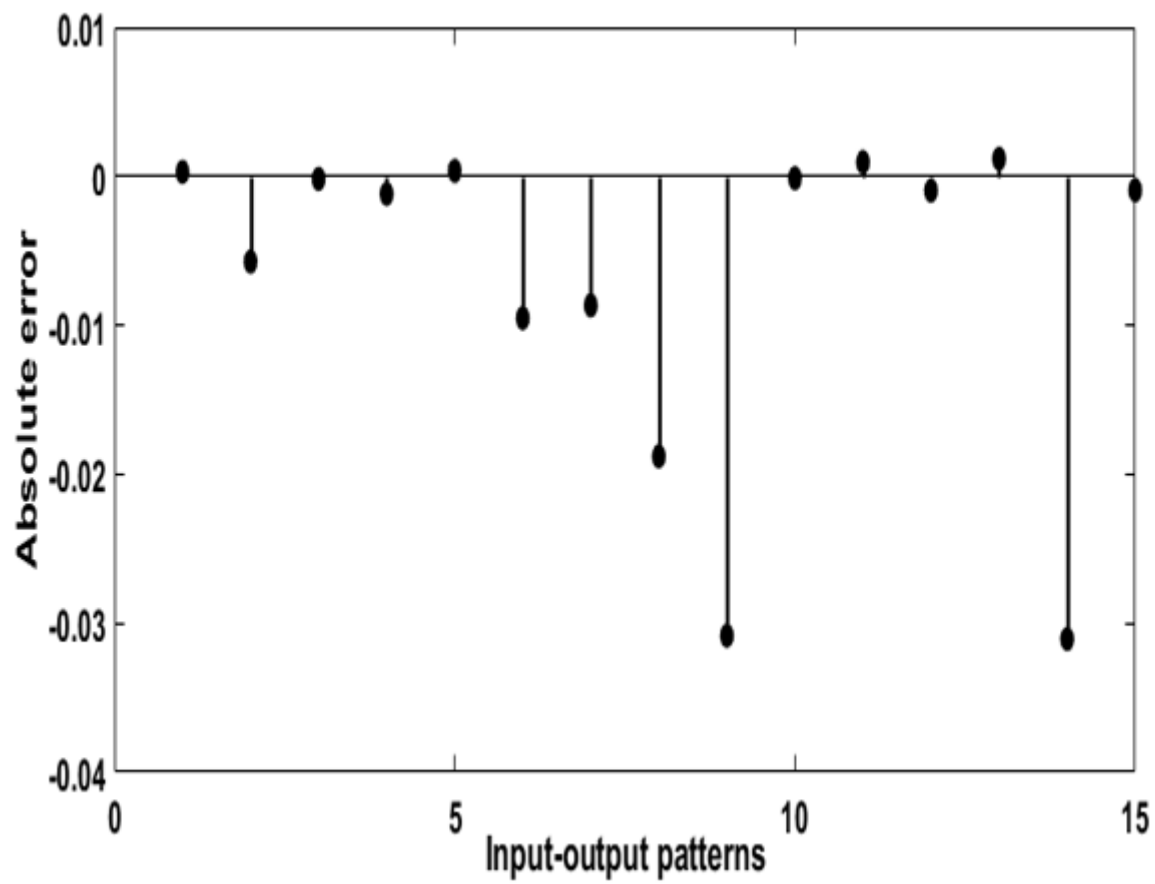
Figure 14

Absolute error related to 'fr'

Figure 15

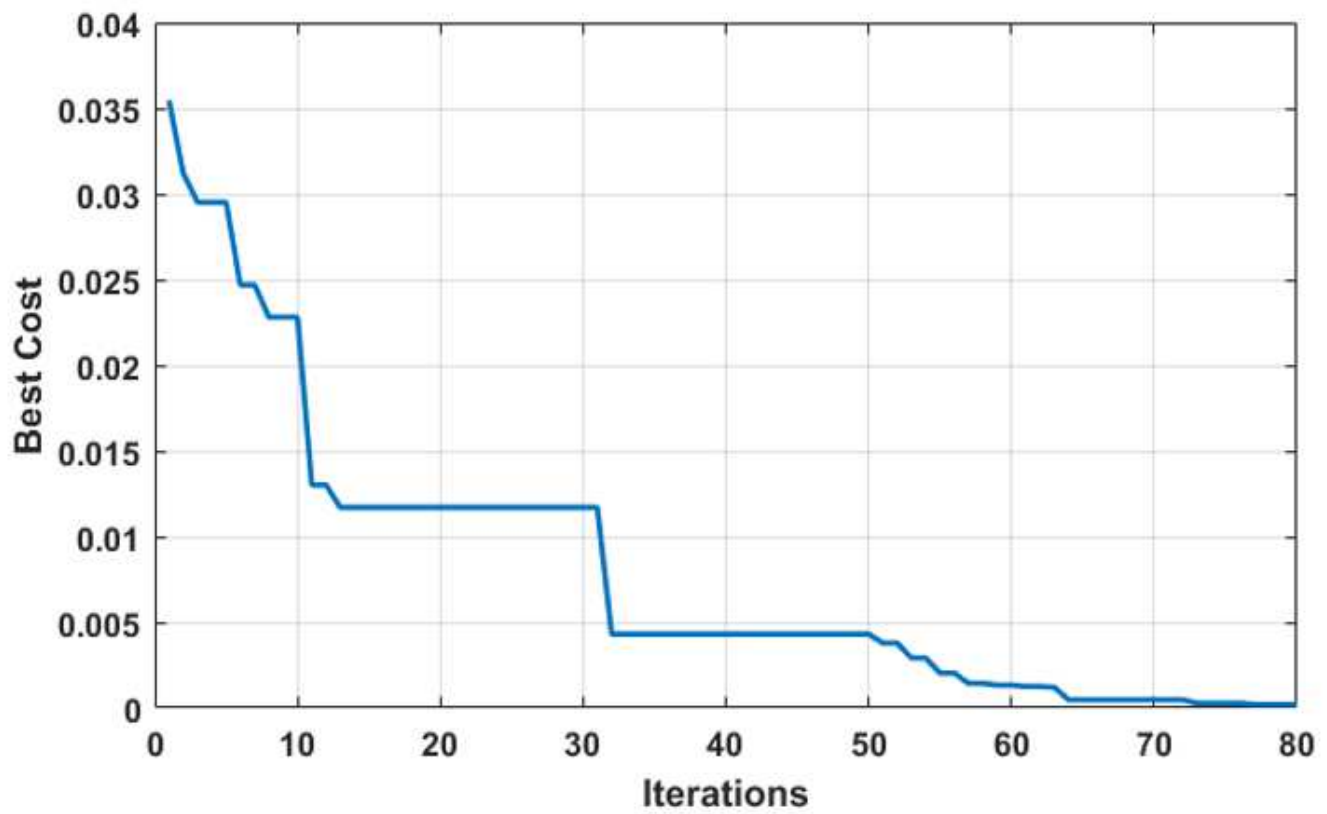Absolute error related to 'g'

Figure 16

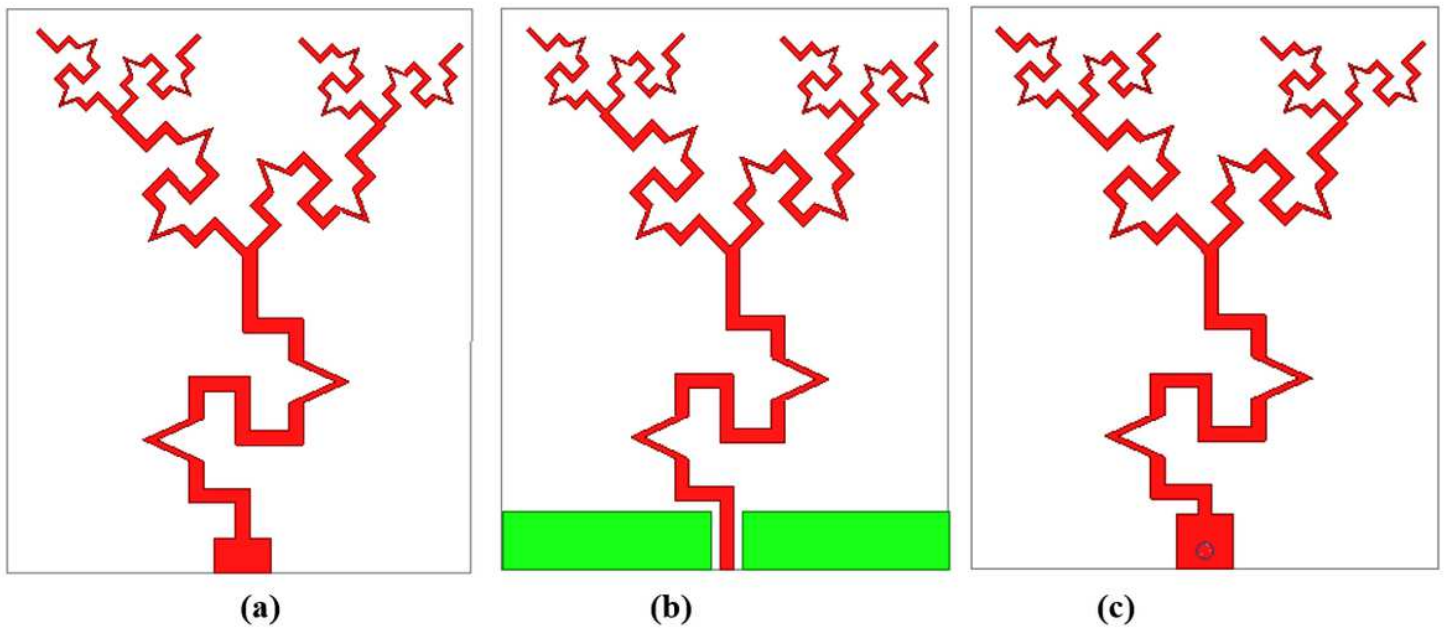Variations of Best cost with iterations

Figure 17

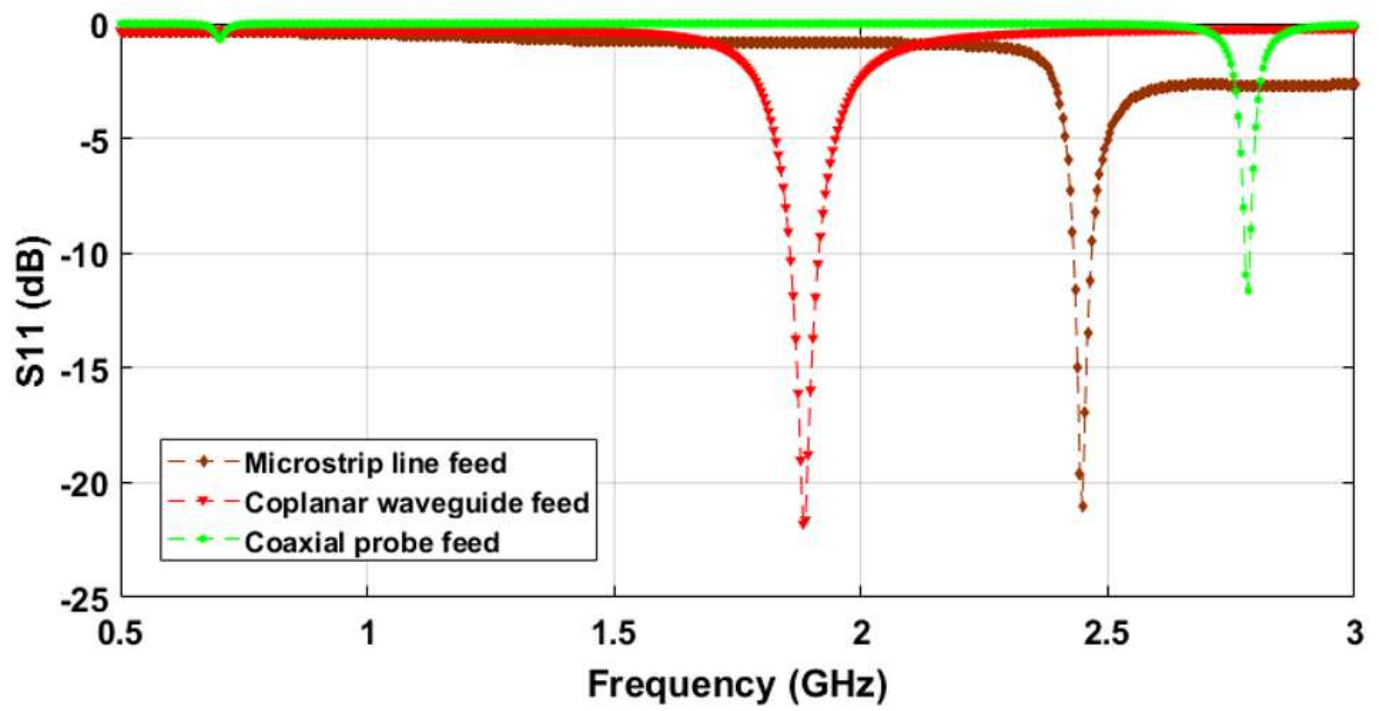Projected antenna with (a) Microstrip line feed (b) Coplanar waveguide feed (c) Coaxial feed

Figure 18

S11 plot with different excitation techniques